

Letter of Transmittal

April 8th, 2021

To:

Dr. Gabriel Potvin

Faculty of Chemical and Biological Engineering

University of British Columbia

V6T 1Z3

Dear Dr. Potvin,

We are submitting our report titled “Optimal Microalgae Biomass Production in Three Types of Cultivation Systems” as a fulfillment of the CHBE 464 Term 2 course requirements. Attached at the end are appendices showing collected data, calculated data and figures, sample calculations and sample error calculations.

This report investigates three types of cultivation systems with the aim of maximizing the carbon dioxide utilization through phototrophic growth of microalgae *C. reinhardtii*. We discuss the various conditions under which experiments were conducted and the significance of the variance in results. We analyzed the data using empirical models to visualize the processes and statistical analysis to determine significance of any variable.

An economic analysis is then conducted to determine if the additional operating costs associated with artificial lighting, temperature control, and aeration control are offset by the increase in biomass yield for each case.

An environmental assessment is then completed to determine if each of the cultivation systems have net positive or net negative carbon dioxide emissions.

We would also like to thank Darien Grace for performing all the experimental work for us during the long laboratory sessions and ensuring that we were aware of any mishaps that may have occurred. We hope that you find this report to meet your expectations.

Sincerely,

Christina Moreno, Jude Abu Namous, Olivia Garland, and Riley Ballachay

CHBE 464

Optimal Microalgae Biomass Production in Three Types of Cultivation Systems

Dates of Experiments:

February 4th, 2021

February 25th, 2021

March 11th, 2021

Date of Submission:

April 8th, 2021

Presented To:

Dr. Gabriel Potvin

Darien Grace

Group 13

Christina Moreno 12506168

Olivia Garland 16973166

Jude Abu Namous 11792165

Riley Ballachay 20266169

Abstract

Conditions of three different large-scale photobioreactors are simulated for growth of *Chlamydomonas Reindhardii*, including an indoor airlift, outdoor tubular reactor and outdoor raceway pond. Six 1-L cultures are set in a temperature-controlled, illuminated environment with regulated control of an air/CO₂ supply to cultures through sparging. Cultures are raised in Tris-Acetate-Phosphate medium for two weeks with varying temperature, illumination and gas flow conditions. To simulate the most significant conditions between the three selected photobioreactors, temperature, light and gas supply conditions are manipulated between experiments. Conditions for 'outdoor' flasks are selected based on average summer conditions in San Diego. Temperature is controlled at 30°C for the 'indoor' experiment, while temperature control is turned off for 'outdoor' reactors - subjecting the flasks to daily variations in indoor temperature. Constant illumination is supplied for the 'indoor' experiment, while a 14/10-hour light/dark cycle is utilized for the 'outdoor' experiments. Light was supplied at approximately 7000 lux for the indoor airlift and tubular bioreactors, and 5000 lux for the raceway pond to account for differences in reactor geometry. A range of gas flows are investigated across experiments, from a high of 0.9 L/min to a low of 0.4 L/min. All gas is supplied with a uniform ratio of 5% CO₂ (v/v) to account for changes in pH. Cell density is quantified using spectrophotometric analysis at 750 nm and calculating the dry cell weight using a cell mass calibration curve. Statistical analysis is performed between replicate flasks using the Mann Whitney U-test and between conditions using Student's t-test using a significance level of $\alpha=0.05$. Maximum cell density over two weeks of cultivation is 3.6 (± 0.4), 3.4 (± 0.2) and 1.7 (± 0.3) g DCW/L for the 'indoor airlift', 'outdoor tubular' and 'outdoor raceway' bioreactors, respectively. No statistical significance is found between the first two condition sets, while the third is significantly different than the first two. Maximum growth rate for the three condition sets is calculated from the first four days of growth and is determined to be 1.46 (± 0.02), 1.20 (± 0.06) and 1.11 (± 0.05) day⁻¹. Growth rate is found to be significantly different between each condition set. The reported cell densities are higher than average cell densities reported in the literature, especially in large-scale photobioreactors. Growth rates are within the reported range for the literature. Self-shading is found to be a significant factor in affecting growth rates, and recommendations are made for abating this factor in future experiments. A complete economic and environmental analysis between the investigated reactor types is performed, and the results

are used to make a recommendation on which bioreactor type should be brought to scale based on the experimental results.

Summary of Contributions

Group Member	Contributions
Christina Moreno	Introduction Theory Experimental Apparatus and Design Lab Calculations
Jude Abu Namous	Letter of Transmittal Nomenclature Recommendations and Implementation of Solution Conclusion Lab Calculations – Economic Analysis & Environmental Assessment
Olivia Garland	Objectives Appendix A, D Lab Calculations
Riley Ballachay	Abstract Results & Discussion Conclusion Lab Calculations

List of Tables

Table 1: Experimental Design Conditions	5
Table 2: Maximum growth rate at each flask location over all three experiments.	10
Table 3: Capital expenditures (CAPEX) for each cultivation system [26]	15
Table 4: Operating expenditures (OPEX) and energy consumption estimates for each cultivation system [26]	16
Table 5: Summary of Net Present Value (NPV) analysis	17
Table 6: Summary of energy consumption, CO ₂ emissions, and carbon tax for each experiment	18

List of Figures

Figure 1: Wide range of microalgal biomass applications [2]	1
Figure 2: Dry cell weight calibration curve generated by fellow lab group.	2
Figure 3: Mechanism for CO ₂ uptake by microalgae. Reaction 1 demonstrates how CO ₂ is converted into carbonic acid based on the pH of the growth medium. Reaction 2 is the acid dissociation to HCO ₃ ⁻ . Equation 1 is the available CO ₂ as related to pH of the growth medium and mass transfer rate. Equation 2, 3 are the CO ₂ transfer rate determined by the partial pressure of CO ₂ and gas concentration in the growth media [5].	3
Figure 4: Experimental Apparatus set up in lab [3]	5
Figure 5: Growth curve for each set of conditions. Error bars show difference between max/min of duplicated at each time point.	7
Figure 6: Concentration of CO ₂ as percent of saturation as a function of k _{La} values retrieved from the literature. Saturation concentration of CO ₂ evaluated at 25°C and 1 atm.	8
Figure 7: Average growth rate from each based on 6 replicates with variable gas flow rate and calculated from expansion between days 0-4 of cultivation.	9
Figure 8: Average light intensity (in lux) at each flask location in the growth cabinet, averaged over three experiments. Flasks are A1, A2, A3, B1, B2, B3 from left to right.	10
Figure 9: Average	12
Figure 10: Estimated penetration depth of light at 750 nm, where penetration depth refers to depth at which light reaches saturation irradiance for C. . Inoculation and maximum densities based off experiment 1.	13

Nomenclature

Symbol	Unit	Description
GHG	-	Greenhouse gas
OD ₇₅₀	-	Optical density at 750 nm
R ²	-	Coefficient of Determination
k _L a	s ⁻¹	Gas Transfer Coefficient
Y _{X/CO2}	-	Yield of Biomass on CO ₂
μ	day ⁻¹	Specific Growth Rate
I	lux	Light Intensity
TAP	-	Tris-Acetate-Phosphate
CAPEX	\$	Capital Expenditures
OPEX	\$/yr	Operating Expenditures

Table of Contents

Letter of Transmittal	i
Abstract	iii
Summary of Contributions.....	v
List of Tables	vi
List of Figures	vi
Nomenclature	vii
Introduction.....	1
Theory	2
Objectives.....	4
Experimental Design and Apparatus.....	5
Results, Discussions and Recommendations	6
Recommendations and Implementation of Solution.....	11
Economic Analysis	14
<i>CAPEX</i>	11
<i>OPEX</i>	12
<i>Net Present Value (NPV) Analysis</i>	13
Environmental Assessment	14
Scale-up Considerations & Recommendations	15
Conclusion	20
References	22

Introduction

The ever-increasing amount of greenhouse gas (GHG) emissions perpetuate the global warming crisis by contributing to the change in climate. Sustainability efforts have gained mainstream media attention forcing people to reconsider their resourcefulness and to shine a light on lax corporation emission standards. Carbon dioxide (CO₂) is the primary greenhouse gas emitted by human activity contributing to 81% of total GHGs [1]. By just reducing the amounts of CO₂ emitted into the atmosphere, the overall GHGs would drastically decrease and improve the current climate crisis that looms over our high-consumer based lifestyle.

Microalgae are single-cell photosynthetic organisms that use CO₂ to produce an algal biomass with a wide variety of applications. The figure below shows the various industry sectors where the biomass can be used once processed. With so many different possible applications, there is increased interest in the use of microalgae as an efficient resource recovery method due to lost cost of cultivation. Concerns about the scale-up feasibility and cost effectiveness stifle the potential success of microalgae and therefore optimization of large-scale cultivations is required before wide-spread use.

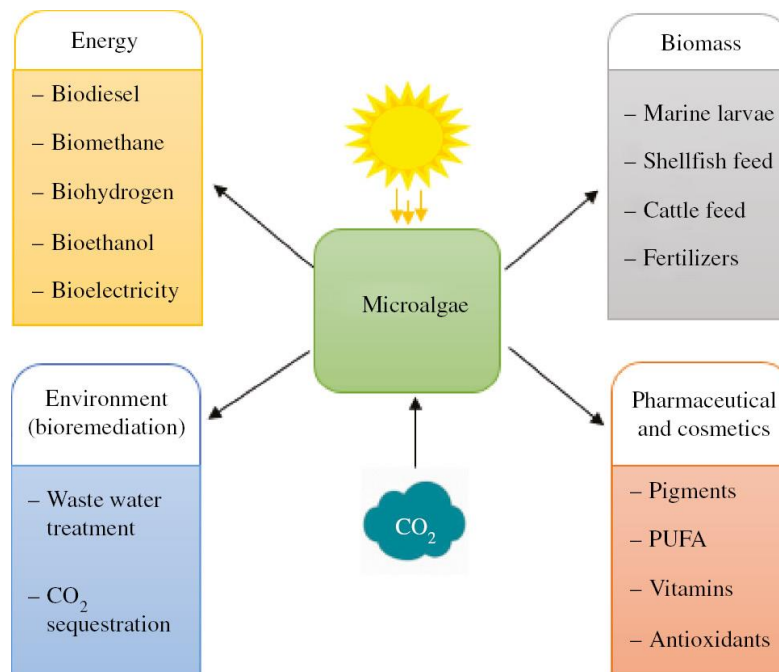


Figure 1: Wide range of microalgal biomass applications [2]

Due to emission concerns, our engineering firm has been hired by a company to optimize the conversion of their CO₂ emissions by way of microalgae biomass production without operating

at a loss [3]. In this experimental design, we investigated the economics of three prominent microalgae cultivations systems by simulating their operating conditions in a lab-scale apparatus where the microalgae *Chlamydomonas Reinhardtii* was cultivated in tris-acetate-phosphate (TAP) media. Results were analysed using the Mann Whitney U-test and parameter conditions used to simulate each system were found through relevant literature review.

Theory

Microalgae are unicellular microorganism capable of performing photosynthesis using CO₂ sunlight and water. *C. Reinhardtii* is a single cell green alga commonly used for cell and molecular biology research, termed the green yeast for its model of fundamental processes [4]. Like classic bacterial cell growth, the optical density is related to the dry cell weight of a sample by the following calibration curve.

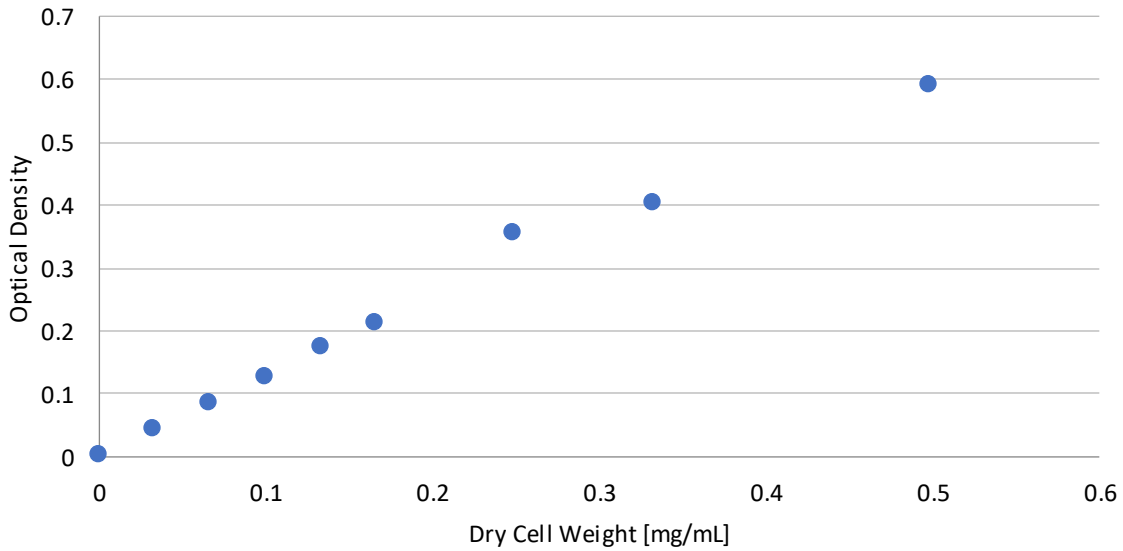


Figure 2: Dry cell weight calibration curve generated by fellow lab group.

By relating the measured OD₇₅₀ values to the dry cell weights, the cell concentrations over the experimental run time were found and growth rates were determined using a modified Monod equation that relates the light intensity to the specific growth rate.

$$\mu = \mu_{max} \times \frac{I}{K+I} \quad (1)$$

Where μ and μ_{max} are the specific growth rate and maximum specific growth rate, respectively, I is the light intensity measured in lux and K is a constant.

Similar to other microalgae species, *C.reinhardtii* has the ability to use CO₂ as the sole carbon source, otherwise known as phototrophic growth. The mechanism of CO₂ uptake depends on gas-liquid mass transfer resistance and soluble amounts of CO₂ in the culture medium. The following set of reaction equations reported by F.A. Almomani can be used to quantify the yield of biomass on CO₂ levels in the system [5]:

$$\begin{aligned} \frac{dC_{CO_2(t)}}{dt} &= k_1 a_{CO_2} (C_{CO_2}^* - C_{CO_2}) - Y_{X/CO_2} \mu X \\ CO_2 + H_2O &\leftrightarrow H_2CO_3 (l) \quad k_H = \frac{[H_2CO_3]}{P_{CO_2}} \quad (\text{Reaction 1}) \\ H_2CO_3 (l) &\leftrightarrow H^+ + HCO_3^- (l) \\ k_{a_1} &= \frac{[H^+][HCO_3^-]}{[H_2CO_3]} \quad (\text{Reaction 2}) \\ IC &= [H_2CO_3] + [HCO_3^-] = k_H P_{CO_2} \left\{ 1 + \frac{k_{a_1}}{[H^+]} \right\} \\ \frac{dC_{CO_2}}{dt} &= \\ k_1 a_{O_2} \sqrt{\frac{D_{CO_2}}{D_{O_2}}} &\left\{ k_H P_{CO_2} \left\{ 1 + \frac{k_{a_1}}{[H^+]} - C_{CO_2} \right\} - Y_{X/CO_2} \mu X \right\} \end{aligned}$$

Figure 3: Mechanism for CO₂ uptake by microalgae. Reaction 1 demonstrates how CO₂ is converted into carbonic acid based on the pH of the growth medium. Reaction 2 is the acid dissociation to HCO₃⁻. Equation 1 is the available CO₂ as related to pH of the growth medium and mass transfer rate. Equation 2, 3 are the CO₂ transfer rate determined by the partial pressure of CO₂ and gas concentration in the growth media [5].

Khan et al. reported that 1 kg of algal biomass can consume 1.83 kg of CO₂ and that CO₂ constitutes 50% of the biomass dry weight [6] which would significantly aid in the diminishing GHG emissions of fossil fuels by providing an eco-friendly method of fixing the global CO₂ problem.

Three biomass cultivation systems that have proven to produce high levels of biomass output are the indoor airlift bioreactor, the outdoor tubular reactor and the outdoor raceway pond. By maximizing the biomass produced by the cultivation of microalgae, more CO₂ is consumed per batch thereby significantly reducing the CO₂ released into the atmosphere. Additionally, more downstream purification options are attainable with higher biomass yields, leading to more potential for sustainable product development.

Indoor airlift bioreactors are the “optimal” condition where the microalgae growth occurs in temperature controlled irradiated chambers. Rather than using traditional methods of mixing, this

system takes advantage of an air pump where the injected air dissipates steady state inducing mixing in confined spaces [7]. This type of system has increased gas-liquid interface contact hence promoting CO₂ transfer to the liquid. Additionally, this system does not cause shear damage to cells which promotes high biomass yields by way of higher cell densities in the system.

Outdoor tubular bioreactors rely heavily on environmental conditions but have the highest photosynthetic efficiencies and maximize gas entrainment [8]. This system contains three major components: an airlift pump, gas-separator and transparent reactor tubing running parallel [9].

Outdoor raceway ponds also rely heavily on environmental conditions and have much lower light penetration than the previously mentioned systems. Raceway ponds consist of a closed loop recirculation channel about 0.3m deep where the culture is agitated by a paddle wheel [10]. They are the most used and cheapest cultivation system for commercial production of microalgae [8]. This system operates with high volumes of water and low cell concentration where the water temperature is uncontrolled [9].

Objectives

The overall goal of our study is to determine which conditions would maximize the carbon dioxide utilization in bioreactors, therefore minimizing emissions to the environment. This big picture goal can be broken down into three objectives. The first objective is to simulate conditions of the three bioreactor types which are an indoor lab-scale airlift reactor, an outdoor tubular bioreactor and an outdoor raceway pond. This first objective will be completed by performing literature review and developing an understanding of each system so that their conditions can be transferred to our experimental set up.

The second objective is to determine effect of light intensity, temperature, and aeration rate on biomass yield. This is performed by taking quantitative measurements of optical density over a period of two weeks for each set of conditions and performing statistical testing to determine which effects are significant. After determining desired set of light temperature and aeration conditions, the final objective is to perform an economic analysis to determine if the increase in biomass yield offsets additional operating costs associated with such conditions. This final objective is met by calculating for operating and capital costs, then performing a net present value analysis.

As the big picture goal of this work is to minimize emissions to the environment, an environmental assessment will also be performed on each reactor type.

Experimental Design and Apparatus

Available to us is a lab-scale set up, seen in Figure 4 below, where the light chamber contains six individually controlled lights, a temperature control system and individualized air streams for the six flasks in the system. Each flask operates with its respective CO₂ and air flow rates.

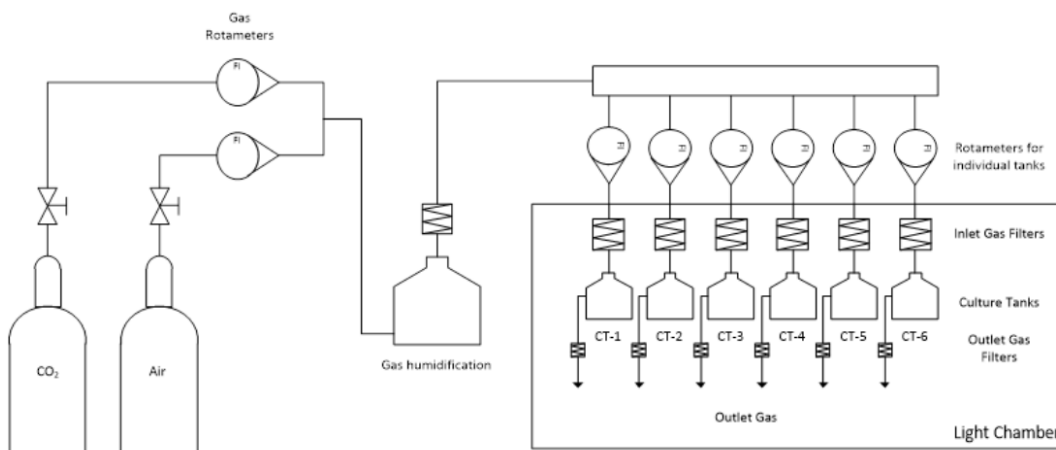


Figure 4: Experimental Apparatus set up in lab [3]

Each experimental day and the following two-week period are dedicated to a single reactor design where samples are collected roughly every 3 days and their optical density is recorded to track growth. Table 1 below outlines the varied conditions to simulate the three-cultivation systems in the lab-scale set up available to us. Prior to each experimental set up, the optical density of the inoculum is recorded to determine the volume added to each flask ensuring equal initial concentrations for all experiments.

Table 1: Experimental Design Conditions

Experiment Day	Cultivation system	Light Settings	Temperature	Aeration
1	Indoor Airlift	6 Lights	30° C	0.8 - 0.6 L/min
	Bioreactor	24 hours		
2	Outdoor Tubular	6 Lights	25° C	0.9 - 0.7 L/min
	Reactor	14 hours		
3	Outdoor Raceway	2 Lights	25° C	0.6 - 0.4 L/min
	Pond	14 Hours		

The microalgae strain *Chlamydomonas Reindhardii* is utilized throughout. Tris-Acetate-Phosphate (TAP) media is prepared according to the provided protocol and used throughout all three experiments to ensure identical initial pH. As the microalgae accumulates and produces various metabolites, the pH is expected to increase but no changes will be made due to the complexity of such a task given the apparatus limitations. Therefore, pH measurements are taken at the start and end of each experiment as a comparison. The maximum airflow rate for all 6 flasks has a maximum limit of 5 L/min therefore flowrates for each flask was adjusted such that the total was below this limit. Since the outdoor tubular reactors operates at maximal airflows, the high and low limits are the upper bounds allowable such that the sum of the flow rates of all 6 flasks equals 5 L/min. The optical density is taken at 750nm for the algal growth tracking and due to time constraints, we have borrowed a calibration curve generously provided to us by our classmates that will be used for data analysis. Light intensity is quantified with a photosensor directly in front of each flask placement to track the luminosity each flask will receive throughout each experiment. Temperature is controlled in only the first experiment at 30°C. For the other two where the temperature is uncontrolled, readings with the thermostat are recorded throughout sample collection for tracking purposes.

Results, Discussions and Recommendations

Cell growth is quantified through spectrophotometric analysis at 750 nm (OD_{750}). A cell mass calibration curve is prepared after recording the OD_{750} values of serial dilution samples of cell suspension and drying a cell sample of known OD overnight and calculating the dry weight. The calibration curve can be found in Appendix A, Figure A-1. The slope of the calibration curve is determined to be $y = 1.190 * OD_{750}$ (mg (DCW)/mL) with R^2 value of 0.996. The curve is then used to calculate dry cell mass from measured values of OD_{750} . While the slope agrees with values reported in the literature, it is common practice to subtract the OD_{750} of the solvent. To compensate for the absence of a solvent blank in this experiment, the intercept was neglected and only the slope was used. Figure 5 shows the cell density of each set of conditions over the duration of cultivation.

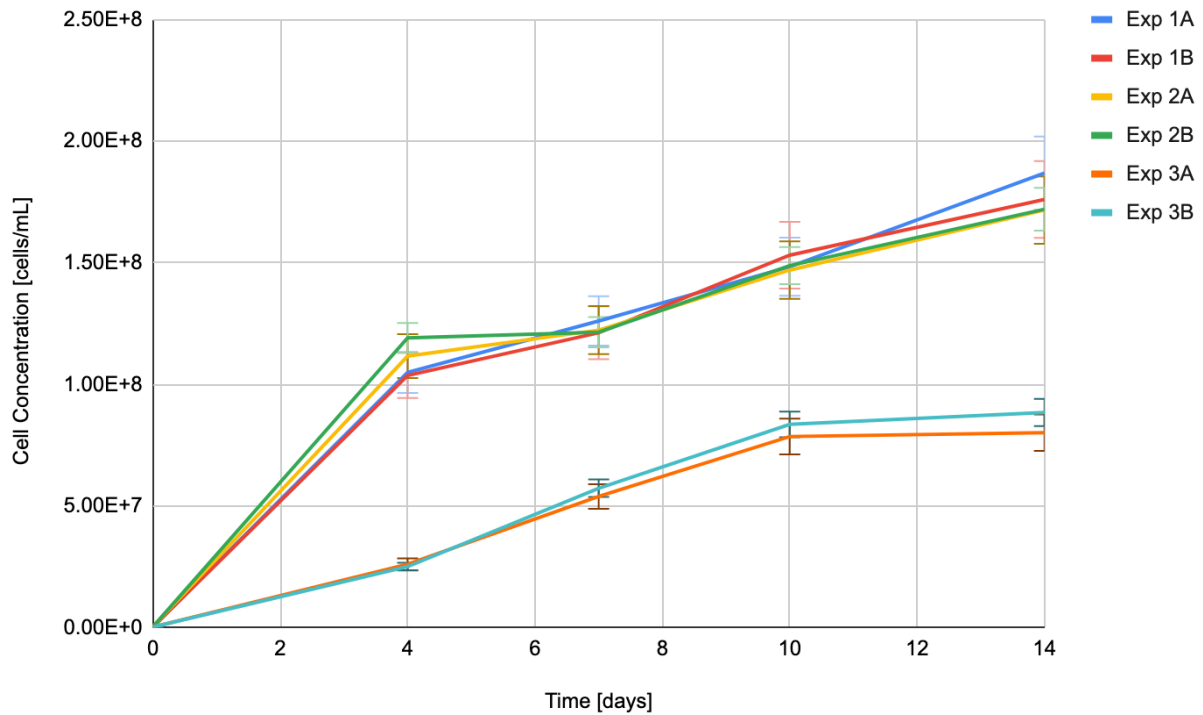


Figure 5: Growth curve for each set of conditions. Error bars show difference between max/min of duplicated at each time point.

All flask conditions are inoculated at approximately uniform density of $3E+05$ cells/mL. Error bars between sub-trial conditions (1A/1B) overlap heavily, signifying that gas flow rate has minimal impact upon growth and final density. To investigate if sub-trial conditions with high/low gas flows may be combined, an investigation into the anticipated effects of varying gas flow rates was performed. Based on the relevant literature, CO_2 sparing in algal culture serves two main purposes: control culture pH by carbonate reaction and drive CO_2 mass transfer between cells and the medium, supplying carbon for photosynthesis [11]. The high and low pH values recorded between all experiments is relatively similar, and all pH measurements fall between 7-7.5. A study which investigated a range of superficial gas velocities overlapping with the current study and 5% v/v CO_2 (similar to 6% utilized in this study) produced a range of gas transfer coefficients (k_{La}) [12]. These results, into addition to an experimental yield of biomass on carbon dioxide ($Y_{X/CO_2} = 0.656$) were used to evaluate a range of possible gas transfer rates in the medium during this experiment, to determine if the culture drops into CO_2 -limited growth (<70% saturation) [13]. Figure 6 shows the estimated concentration of CO_2 in the culture based

on the highest maximum growth rate observed over all experimental conditions, and the range of k_{La} values provided in the literature:

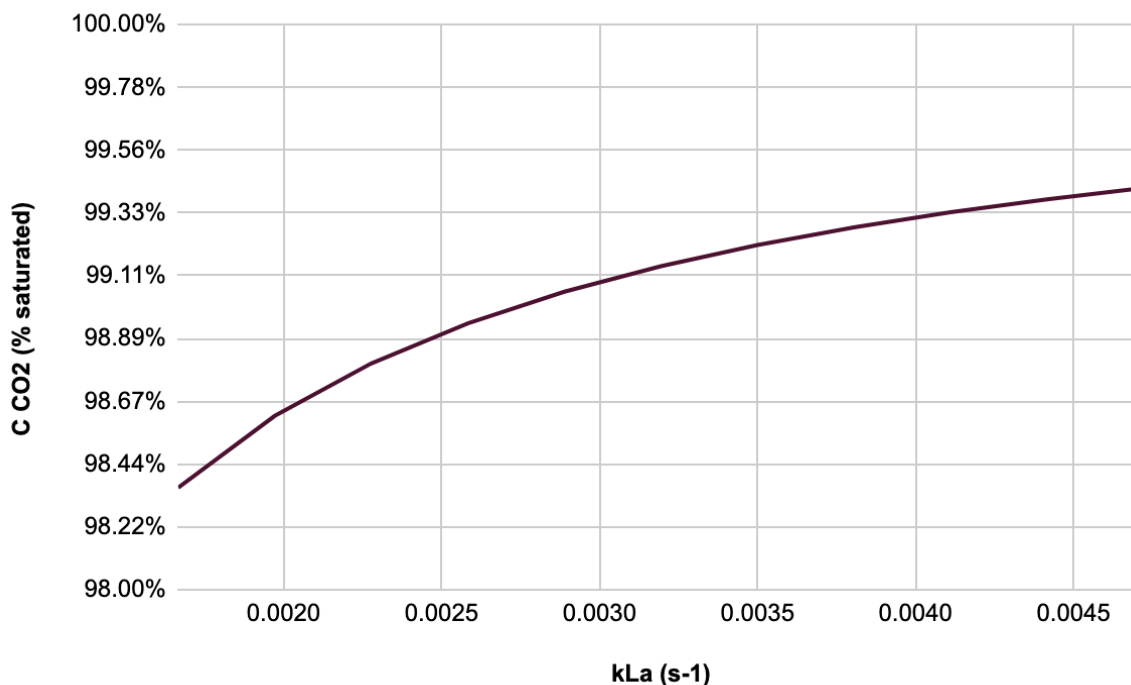


Figure 6: Concentration of CO₂ as percent of saturation as a function of k_{La} values retrieved from the literature. Saturation concentration of CO₂ evaluated at 25°C and 1 atm.

The results of this analysis affirm the predominant opinion in the literature, and this experiment, that CO₂ is rarely a growth-limiting substrate. From here on, sub-samples with variable gas flow rate are grouped together to make more robust conclusions from the results. It is important to note that this assumption is more relevant for experiments 1 and 2. Mixing should, in theory, have a more pronounced effect on lower-light cultures, as light does not penetrate as far into the culture, and cells must be cycled out to the perimeter of the flask to be fully illuminated and photosynthesize [14]. The most common growth model for algal cultures is the Monod model altered to be a function of light intensity [15]. Using this knowledge, and the assumption that the culture is being light-unlimited for the first four days of the culture, a log-log plot is used to estimate the maximum growth rate. The first four days were used, as the log-log plot tapers off significantly in all three experiments after this point. The results from this analysis are shown in Figure 7.

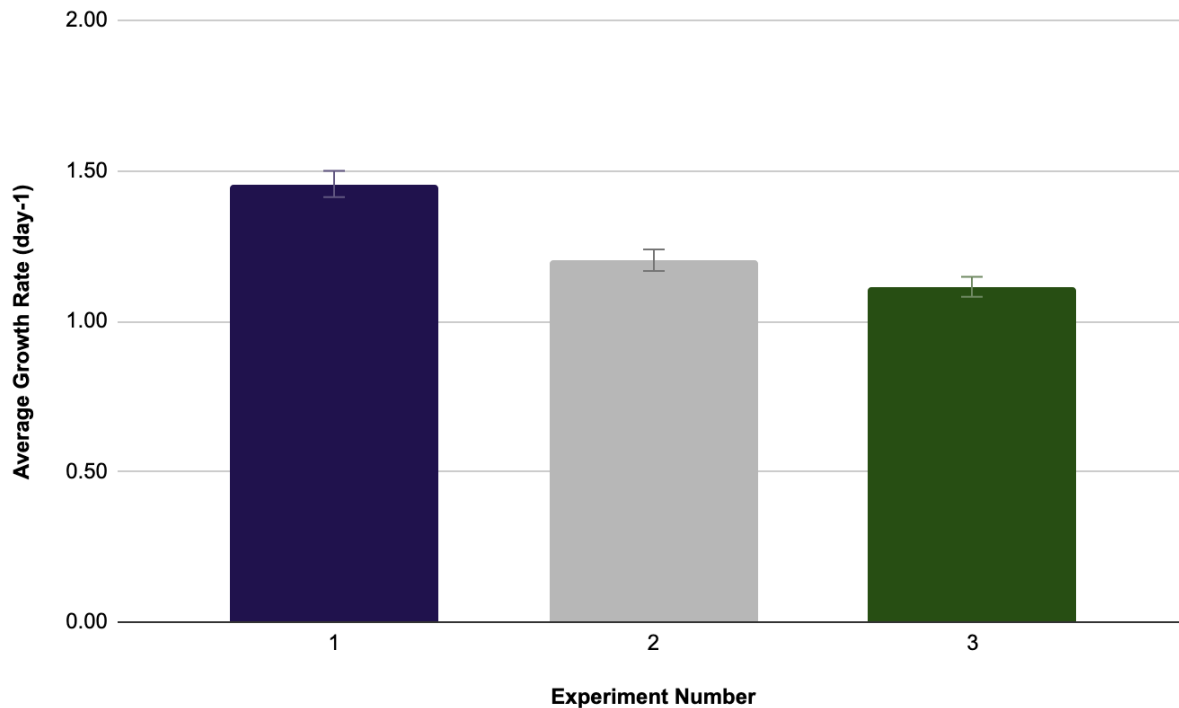


Figure 7: Average growth rate from each based on 6 replicates with variable gas flow rate and calculated from expansion between days 0-4 of cultivation.

It is important to acknowledge the large source of error introduced into growth rate calculated only using two data points for two reasons: estimating the linear regression coefficient using two data points is extremely inaccurate, and similar experiments in the literature observed light-limited growth within 3 days of culture. This indicates that there is a high probability that the growth rate reaches a maximum and begins to decrease within the first four days of culture, and the estimated value is lower than true maximum growth rate [16]. Student's t-test is performed between each pair of conditions, and all growth rates are determined to be significantly different with a significance of $\alpha=0.05$. Observed growth rates are similar to values reported in equivalent experiments with *C. reinhardtii* ($\sim 1.44 \text{ day}^{-1}$) [15]. The difference in growth rates between experiment 1 and 2 is expected to largely be a function of illumination (24 vs 14 hours). The measured difference in temperature between the two experiments was only about 5 degrees (27 vs 22°C), and it has been shown in prior work that the growth of *C. reinhardtii* is weakly dependent upon temperature in this range [17]. It is hypothesized that the difference between growth in experiment 3 and the other two experiments is largely attributable to light intensity:

the average light intensity in experiment 3 is 4211 lux, or ~66% of the 6342-lux observed in the indoor airlift bioreactor, while the growth rate is ~76% of that observed in experiment 1. As previously described in the experimental design section, flask placement was chosen in effort to ensure that each flask received the same light intensity. A staggered flask placement was chosen, but exploration into whether the difference in light intensity which reached each flask was necessary to decide whether our triplicates were truly comparable for the remainder of the analysis. Light intensity measurements were taken at each flask location in the cabinet on the first and last days of the 2-week cultivation period. Figure 8 shows the approximate location of each flask within the cabinet and the average light intensity (in lux) recorded at each flask location averaged over all three experiments.

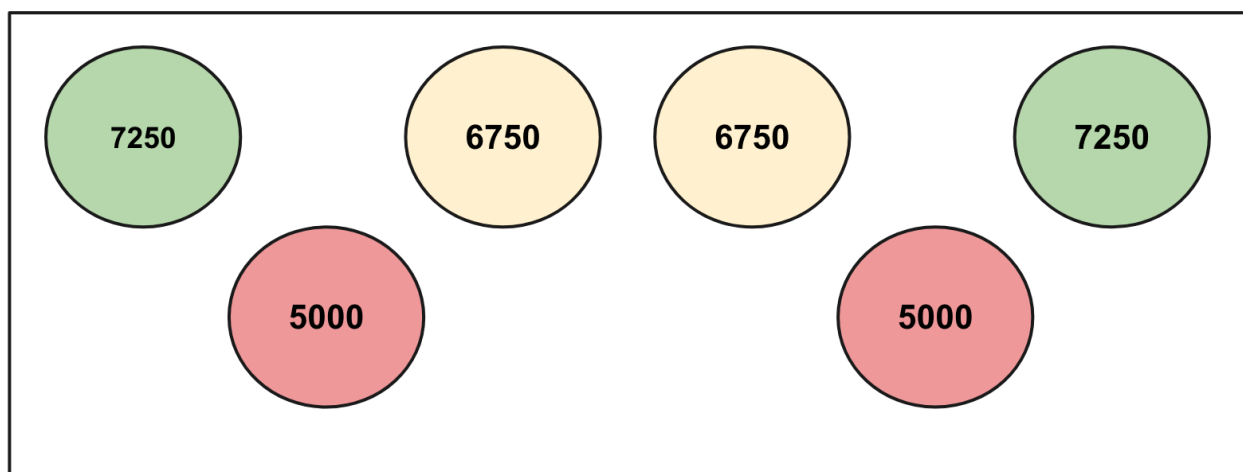


Figure 8: Average light intensity (in lux) at each flask location in the growth cabinet, averaged over three experiments. Flasks are A1, A2, A3, B1, B2, B3 from left to right.

In addition to analyzing the average lux at each location, the results indicated that flasks in locations indicated in red in Figure 4 had substantially lower final cell density than those indicated in yellow and green. Averaged over all three experiments, flasks located in positions A2 and B2 had 85% of the final cell density as the other flasks. A similar but much less distinct trend was observed when comparing maximum growth rate between flasks.

Table 2: Maximum growth rate at each flask location over all three experiments.

Location	A1	A2	A3	B1	B2	B3
Light (lux)	7250	5000	6750	6750	5000	7250
μ (day-1) - Exp 1	1.48	1.44	1.46	1.43	1.44	1.49
μ (day-1) - Exp 2	1.15	1.13	1.26	1.21	1.19	1.28
μ (day-1) - Exp 3	1.15	1.04	1.12	1.17	1.08	1.13

These results agree strongly with Monod model of growth for *C. reinhardtii*. The maximum growth rate observed in the literature for this strain of algae is approximately 1.5 day^{-1} , indicating that growth rates observed on day 1 are close to the μ_{max} attainable, and that cells are supersaturated with light [18]. As the average μ decreases across experiments, the effect of flask location is more pronounced. μ is 98%, 95% and 92.5% lower, on average, at the low-light locations moving from experiment 1 to 3, respectively. The trend in maximum cell density is much more pronounced, and to determine if the mean final cell density at these locations is statistically different, the Mann-Whitney U-test was performed. This test was chosen as it is appropriate for small sample sizes that are non-normally distributed [19]. Flasks within higher intensity locations (Samples A and C) were grouped and compared against Sample B. The test determined that there was a significant difference between the final dry cell weight between the groups. The same test was performed between the samples A and C and no significant difference was found.

In response to the statistical significance between the maximum cell density observed in flasks A2/B2 and the other replicates, those replicates are discarded from analysis of final cell density. Another source of error impacting the quality of the data in this part of the analysis is an experimental error, in which the gas flow was accidentally turned off for two days in the second week of growth in the first experiment. To counteract this error, the samples were grown for an additional two days. Owing to prior analysis indicating that gas isn't as significant a factor as light, however, it was decided that experiment 1 would still be analyzed on the 14th day. Figure 5 shows the final cell density of all three experiments.

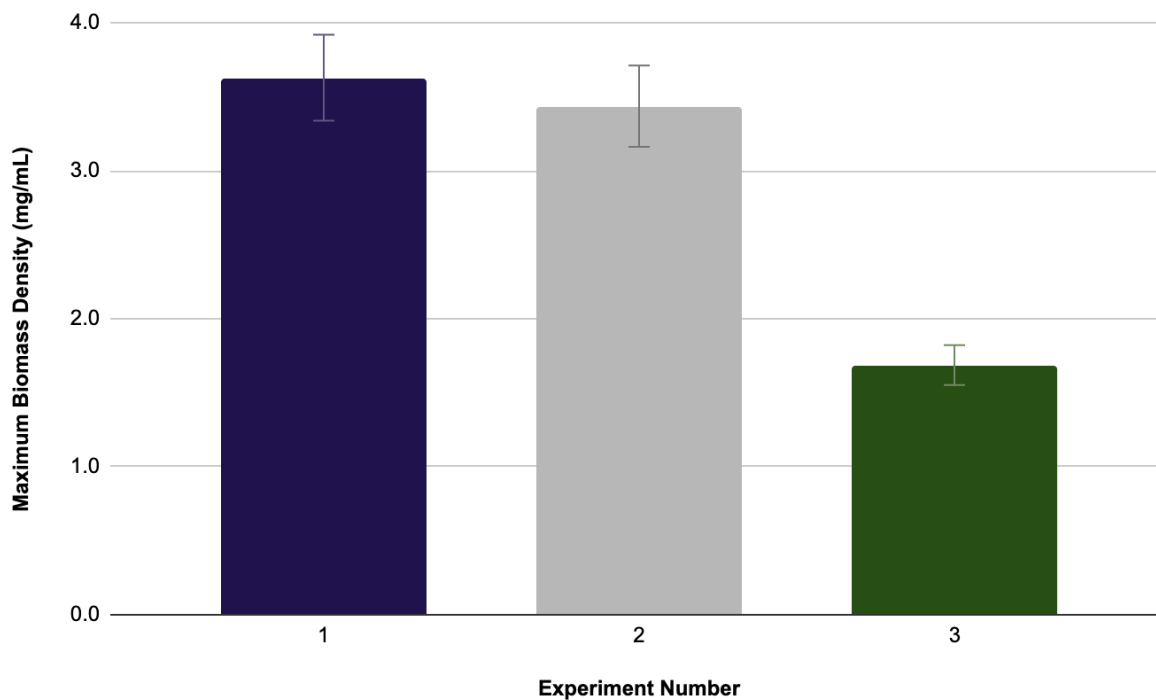


Figure 9: Average maximum biomass density observed between experiments. Four replicates shown for each bar.

Maximum density achieved in experiments 1 and 2 were not determined to be significantly different with at a significance level of $\alpha=0.05$. Experiment 3, however, was determined to be significantly different than both with the same degree of significance. There are a few possible explanations for the similar final density in experiments 1 and 2. Mixotrophic cultures, where algal cultures are subjected to an extended period of darkness daily in the presence of a catabolizable carbon source (provided in this experiment by the TAP media), have shown to sustain higher densities than purely autotrophic cultures [20]. It is also possible that the marginal gains provided by constant illumination vs. 14 hours/day, while they increased the maximum growth rate, were slowly eaten up as the effects of self-shading began to dominate growth after roughly the fourth day of cultivation. Self-shading is the phenomenon whereby an algal culture becomes too dense for light to be able to penetrate the culture and is the most-significant hurdle to engineers during the scale-up of photobioreactors [21]. It is also the reason why production-scale cultures rarely sustain densities higher than 1 g/L, about 4x lower than those reached in this experiment [22].

From Figure 5, a significant decline in growth rate is observed following day 4 in all samples. To determine if this is the result of self-shading, a review of experiments which estimated the penetration depth of light in algae cultures was performed. The most common technique employed in these papers is to assume that light provided in the experiment is distributed across wavelengths similarly to sunlight, and that the assumptions of Beer's Law hold [23]. Using the culture absorbance at 750 nm, the 'penetration depth' can be calculated as the point at which the light intensity drops below the saturation intensity of *C. Reinhardtii*, 1.4 pW/ μm^2 [21]. Figure 6 shows the cell concentration and estimated penetration depth of light at 750 nm, with the inoculation, break-even and maximum cell densities indicated. Break-even is the point at which the center of the flask (radius ~50 mm) drops below saturation irradiance, assuming light enters perpendicular to the radius of the flask.

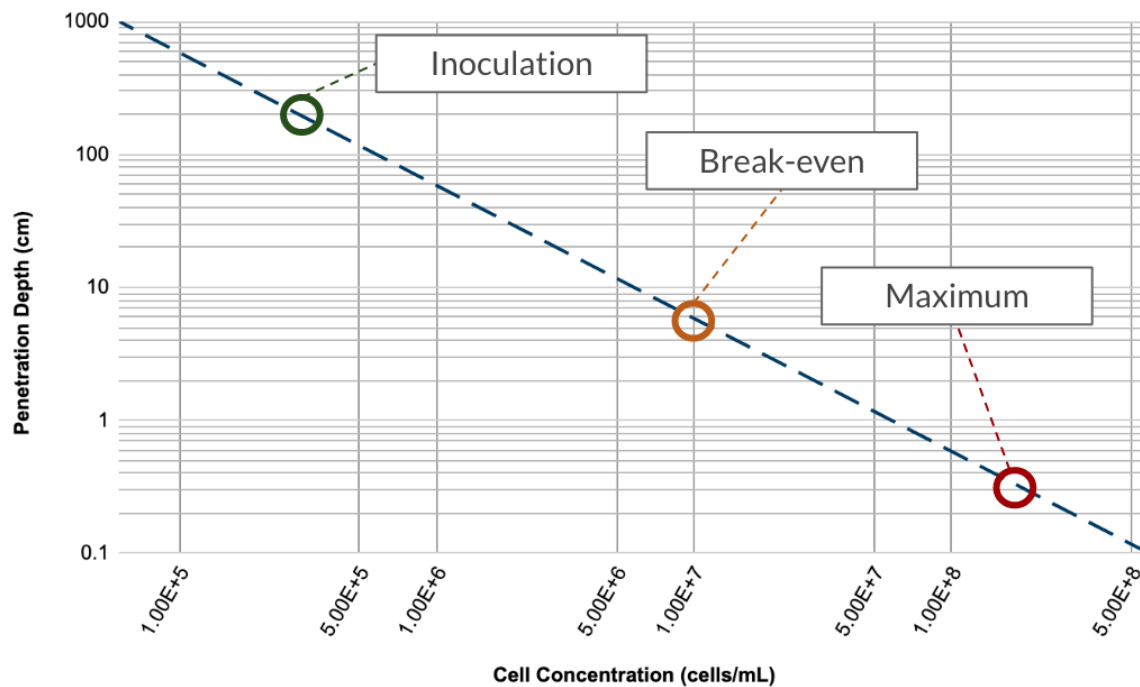


Figure 10: Estimated penetration depth of light at 750 nm, where penetration depth refers to depth at which light reaches saturation irradiance for *C. Reinhardtii*. Inoculation and maximum densities based off experiment 1.

These results strongly indicate that self-shading is playing a significant role in controlling the growth rate throughout the experiment, and therefore significantly reduces the significance of the results obtained from this experiment. The break-even density is reached in all cultures, as shown on Figure 1, prior to day 4. This indicates that all growth rates calculated are likely an under-

estimate of their true value. By the final day of growth in experiments 1 and 2, light is only penetrating approximately 0.3 cm into the culture. This indicates that the true discrepancies between the cultivation styles are incredibly overshadowed by the effects of self-shading, and the low sampling frequency in the first few days. The geometry of bottle (cylindrical) and style of cultivation (batch) utilized in this experiment is also a significant source of error when attempting to extrapolate to production scale, as most bioreactors use complex geometries and steady-state dilution to maintain an optimal cell density and negate the effects of significant self-shading [24, 25].

Recommendations and Implementation of Solution

Economic Analysis

Each of the three cultivation systems described in this report have respective advantages and disadvantages as described previously. Our experiments indicate that additional investments in controlling light and temperature result in a statistically significant increases in algal density, and CO₂ utilization. While the additional levels of control in these parameters result in greater yields, they also necessitate higher capital and operating costs. As engineers, it is necessary to understand this trade-off and determine whether the revenue generated from the additional biomass produced is offset by the additional operating costs associated with higher levels of control. One way this analysis is performed during a normal phase of engineering design is through a Net Present Value (NPV) analysis.

The methodology for conducting the economic analysis is described in this report. However, due to the lack of data available for cost of equipment, some major assumptions have been made, and therefore no definitive conclusions can be made based on our economic analysis. It is recommended that more research into equipment costs is conducted prior to repeating the same economic analysis outlined in this report.

CAPEX

The capital expenditures (CAPEX) for each experiment are outlined in Table X below. The costs used for the CAPEX are taken from a similar study done in Thailand [26].

Table 3: Capital expenditures (CAPEX) for each cultivation system [26]

	Experiment 1	Experiment 2	Experiment 3
	Indoor Airlift Reactor	Outdoor Tubular Reactor	Outdoor Raceway Pond
Air pump	\$ 8.53	\$ 8.53	\$ -
Lamps	\$ 171.81	\$ -	\$ -
Bulb	\$ 50.70	\$ -	\$ -
Air conditioner	\$ 463.27	\$ -	\$ -
Capital cost (\$)	\$ 694.31	\$ 8.53	\$ -

One major assumption made when calculating the CAPEX was disregarding the cost of the cultivation system itself. This assumption is not great, but no other direct comparisons of the three cultivation systems has been performed in the literature. It is important to acknowledge that the expenses of the system itself is certainly non-negligible, however it varies significantly based on the scale and location of the facility. A 2012 economic comparison of an Outdoor Tubular Reactor and Open Raceway Pond in Southern USA estimated that CAPEX costs for each system would be approximately \$970 and \$375 million, respectively [27]. Of the capital costs for the PBR system, the tubing system itself accounted for approximately 50%, or \$500 million. The NPV of the Tubular system in this analysis ended up being approximately 3x lower than that of the raceway pond. Another capital expense neglected in this analysis is land cost. Because of the geometry, raceway ponds can require up to 10x more land to achieve the same level of production [28]. This factor alone is a huge barrier to scale-up for raceway ponds. To achieve biodiesel production rate of an average oil well (10,000 barrels/day) in an open raceway pond, an area of 6,000-25,000 football fields would be required. The large area required for this style of cultivation is largely attributable to self-shading. While PBR tubes may be made incredibly thin and stacked dozens of feet high, open raceway ponds can only be about 30 cm deep in practice. According to the plot prepared in the Results section estimating penetration depth based on biomass density, this correlates to a biomass density of 1E+6 cells/mL before self-shading significantly hinders growth. This agrees strongly with the optimal cell density for this style of bioreactor reported in the literature [29]. Biomass is controlled at the target density in both PBR and raceway systems using a biomass harvesting system. This expense is relatively uniform between cultivation systems but can comprise a significant portion of CAPEX expenses (21% for a raceway pond) [28].

OPEX

The operating expenditures associated with each experiment is directly proportional to the additional levels of control implemented in each design. Table X outlines the estimated OPEX for each experiment [26].

Table 4: Operating expenditures (OPEX) and energy consumption estimates for each cultivation system [26]

	Experiment 1	Experiment 2	Experiment 3
	Indoor Airlift Reactor	Outdoor Tubular Reactor	Outdoor Raceway Pond
Air pump energy consumption (Wh/day)	0.6	0.6	0.0
Air pump energy cost (\$/yr)	\$ 0.5	\$ 0.5	\$ -
Light energy consumption (Wh/day)	3006	0.0	0.0
Lighting costs (\$/yr)	\$ 2903	\$ -	\$ -
Temperature energy consumption (Wh/day)	107	0.0	0.0
Temperature control costs (\$/yr)	103	\$ -	\$ -
Total energy consumption (Wh/day)	3113	1.1	0.0
Total energy cost (\$/day)	\$ 0.4	\$ 0.0	\$ -
Operating cost (\$/yr)	\$ 125	\$ 0.04	\$ -

Calculations are arbitrarily made on the basis that one operating year translates to 330 operating days per year. Cost for electricity at \$0.12/kWh is based on electricity rates in British Columbia [30]. Additional operating expenses not considered in this analysis, but worth mentioning are maintenance and insurance costs. Because of the considerable expense added with the delicate tubing system in the PBR, the combined insurance and maintenance costs of the system are estimated to be four times higher in open raceway system [28]. One factor which is neglected in an economic analysis but can have a substantial impact on operating expenses is contamination in open raceway ponds. One economic analysis estimated that contamination mitigation solutions, including pond covers and liners can comprise up to 24% annual expenses, and regularly results in a large reduction in algae yield [31].

Net Present Value (NPV) Analysis

To determine whether the additional revenue from the higher biomass produced in experiments 1 and 2 is offset by the higher operating costs, a net present value analysis is conducted. The net present value is the difference between the present value of cash inflows and the present value of

cash outflows over a period. This type of analysis is typically used in investment planning to determine the profitability of a project. A positive net present value indicates that the project is profitable while a negative net present value indicates that the project results in a net loss [32]. The only source of revenue in our experiments is the sale of algal biomass as fish meal at \$0.0003/g [33]. An interest rate of 10% [34] and a lifetime of 15 years are assumed.

Table 5: Summary of Net Present Value (NPV) analysis

	Experiment 1	Experiment 2	Experiment 3
	Indoor Airlift Reactor	Outdoor Tubular Reactor	Outdoor Raceway Pond
Capital costs (\$)	\$ 694	\$ 8.5	\$ -
Operating costs (\$/yr)	\$ 125	\$ 0.02	\$ -
Revenue (\$/yr)	\$ 0.06	\$ 0.05	\$ 0.02
Lifetime (yrs)	15	15	15
NPV	- \$ 519.29	- \$ 8.14	\$ 0.18

Both experiments 1 and 2 result in a negative NPV and therefore are not considered to be profitable. This can be attributed to the higher CAPEX and OPEX in comparison to experiment 3. Additionally, there is minimal value in the additional biomass produced due to the low price associated with microalgae in the form of fish meal. It is recommended to incorporate downstream processing to convert the harvested microalgae into higher value products to increase the NPV for all three experiments and hence possibly result in a profitable process. A more accurate lifetime should be estimated based on the lifetime of the equipment used rather than making an arbitrary assumption. The results shown here agree strongly with a review of financial analysis on the three systems. While indoor systems result in high yields, their high expense means that their analysis is usually limited to smaller-scale experiments, and rarely make their way to a complete economic analysis [35]. The NPV between tubular and outdoor raceway ponds is relatively similar, and more detailed considerations about land, construction and product quality ought to be made before making a definite decision between the two systems.

Environmental Assessment

The main goal of our study is to maximize the carbon dioxide utilization in bioreactors, therefore minimizing emissions to the environment. Microalgae have been recognized for their CO₂ bio-

mitigation potential with the possibility of feeding industrial flue gases to microalgae cultivation systems, thereby decreasing the CO₂ emissions to the environment. However, microalgae-based CO₂ sequestration is currently prohibitively energy intensive, limiting its industrial applications [36]. The sustainability of the process is dependent on the overall energy consumption and emissions of the key operations in the process [36].

Assuming that non-renewable energy sources are being used, there are carbon dioxide emissions associated with energy consumption. The carbon dioxide emissions are quantified based on a 0.41 kg CO₂-eq/kWh emission rate associated with a gas-fired power plant [37]. This may vary depending on the energy source utilized at the power plant (e.g., coal, natural gas, petroleum). Therefore, the carbon dioxide emissions for each experiment are directly proportional to the energy consumption. The net emissions are then calculated based on the emission rate, the energy consumption and carbon dioxide utilization for each experiment. The carbon tax is then calculated based on a \$30/tonne CO₂ tax rate [37]. A summary of the net emissions and carbon tax for each experiment is outlined in Table 6 below.

Table 6: Summary of energy consumption, CO₂ emissions, and carbon tax for each experiment

	Experiment 1	Experiment 2	Experiment 3
	Indoor Airlift Reactor	Outdoor Tubular Reactor	Outdoor Raceway Pond
Total energy consumption (Wh/day)	3113	0.55	0.00
CO ₂ emissions (kg CO ₂ /yr)	421	0.07	0.00
Carbon tax (\$/yr)	\$ 12.6	\$ -	\$ -
Total CO ₂ consumed (kg/yr)	180	205	128
Net CO₂ emissions (kg/yr)	242	-205	-128

Due to the high energy demand associated with the indoor airlift reactor, it produces 242 kg/yr CO₂ emissions. The outdoor tubular reactor and the outdoor raceway pond have net negative CO₂ emissions at -205 kg CO₂/yr and -128 kg CO₂/yr, respectively. While these results cannot be definitively conclusive due to significant assumptions made in this study, the same conclusion regarding the indoor system can be made as in the economic analysis: it should not undergo further investigation as a large-scale algae cultivation system. A more accurate environmental assessment should be conducted when a comprehensive breakdown of the energy consumption for each cultivation system is completed.

Scale-up Considerations & Recommendations

There are several scale-up considerations that are important to acknowledge. The first is that there are many simplifications made in the economic analysis which were necessary to reduce the scope of this work. One important consideration is the implementation of paddlewheels (or a different agitator system) in the raceway system when scaling up to full-scale [36]. Implementing this change requires revisiting the economic analysis and environmental assessment to incorporate the additional costs and CO₂ emissions associated with the agitator system. This will negatively affect the NPV and likely make the outdoor raceway pond a non-profitable process. Secondly, as previously mentioned in this study, the geometry of the bottle utilized in this experiment are not representative of production scale cultivation systems. This is significant for many reasons. Firstly, light can penetrate from all angles in a tubular bioreactor, while it can only penetrate on one face in an open raceway pond. Additionally, because tubular reactors can be stacked vertically, they can be properly illuminated immediately after sunrise, while recessed ponds may only receive direct sunlight a few hours a day due to the angle of the sun relative to the pond [38]. This further complicates the assumption that any outdoor bioreactor should receive sunlight for the same duration of time. The reactors also utilize gas differently: the tubular bioreactor uses gas to carry algae up through the bioreactor, and therefore the time a bubble is in contact with culture prior to reaching the top of the reactor is significantly longer than a raceway pond, which only has the liquid level of the pond to work with. This aspect of raceway ponds may be of significant detriment for the intended application of CO₂ scrubbing from off-gas. While the gas can easily be recirculated in the closed tubular system, a cover system would need to be designed to capture off-gas from open raceway ponds for analysis prior to exhaust. It is recommended that this study be repeated while incorporating typical geometries associated with airlift and tubular photobioreactors to conduct a more accurate comparison of the two systems, and that the off gas is analysed to ensure that adequate CO₂ consumption is occurring.

In the environmental assessment, it is assumed that all carbon dioxide provided is consumed and converted into biomass. However, as discussed in the previous section, the carbon dioxide is provided in excess and therefore the assumption made in the environmental assessment is incorrect. Ideally, the flow rates should be set such that sufficient carbon dioxide is provided

where it is not a limiting nutrient without providing excess to avoid having unreacted carbon dioxide.

The final and most-important scale-up consideration is avoiding self-shading. Evident from the results of this experiment is that self-shading can greatly reduce the efficiency of a microalgae cultivation system. The way this is typically addressed in scaled-up bioreactors is to implement a filtration or flocculation system which can maintain biomass at a density low enough to mitigate this phenomenon. In this analysis, the dilution rate is typically adjusted experimentally while trying to maximize the biomass production rate [39]. While the maximum growth rate can be considered a surrogate for the production rate, it has shown to be significantly impacted by the effects of self-shading in this work. Future experiments should be terminated after the first week, and more samples should be taken, to better analyze the growth characteristics of that system.

Conclusion

This report investigates the effect of different conditions on maximizing carbon utilization in three types of scaled-up microalgae cultivation systems to minimize emissions to the environment. This was done by manipulating the temperature, illumination and aeration conditions in a lab-scale algae cultivation system. The efficacy of the cultivation system is evaluated using maximum growth rate and maximum biomass density. From a thorough review of the literature, it is expected that light will be the predominant factor affecting growth, with peripheral contributions from temperature and aeration. Maximum growth rates were calculated for the exponential phase of growth. Student's t-test is performed between each pair of conditions with a significance of $\alpha=0.05$. Maximum cell density over two weeks of cultivation is $3.6 (\pm 0.4)$, $3.4 (\pm 0.2)$ and $1.7 (\pm 0.3)$ g DCW/L for the 'indoor airlift', 'outdoor tubular' and 'outdoor raceway' bioreactors, respectively. No statistical significance is found between the first two condition sets, while the third is significantly different than the first two. Maximum growth rate for the three condition sets is calculated from the first four days of growth and is determined to be $1.46 (\pm 0.02)$, $1.20 (\pm 0.06)$ and $1.11 (\pm 0.05)$ day⁻¹. Growth rate is found to be significantly different between each condition set. Gas flow rate is found to be an insignificant factor in affecting growth and is neglected as a factor during statistical analysis. Statistical analysis of replicates with varying light intensity is performed using a Mann Whitney U-test, and replicates

are discarded from analysis as a result. A literature search on parameters for a gas-uptake model estimated that carbon dioxide is supplied at 98% saturation at a minimum across experiments. A thorough investigation of the effects of self-shading in the experiments is performed. A Beer's Law analysis of light penetration at 750 nm is used to predict that self-shading becomes a limiting factor after the third day of growth, and independently controls the maximum cell density in the second half of cultivation.

An economic and environmental analysis is used to frame the results from the experiment and determine which scaled-up bioreactors would be feasible. The CAPEX and OPEX costs of the indoor bioreactor are significantly higher than both the outdoor tubular and raceway bioreactors. It is determined that the indoor bioreactor should be removed from consideration due to high expenses. Too many assumptions were made in the economic analysis to decide between the two outdoor systems, it is recommended that a more detailed analysis is undertaken. This would include a more thorough analysis of capital expenses associated with each system and ensuring that the geometry and growth conditions in the two downscaled bioreactors more closely approximate those of the real systems.

References

- [1] Overview of Greenhouse Gases. EPA. [https://www.epa.gov/ghgemissions/overview-greenhouse-gases#:~:text=Carbon%20dioxide%20\(CO2\)%20is,gas%20emitted%20through%20human%20activities.&text=Larger%20image%20to%20save%20or%20printThe%20main%20human%20activity,changes%20also%20emit%20CO2.](https://www.epa.gov/ghgemissions/overview-greenhouse-gases#:~:text=Carbon%20dioxide%20(CO2)%20is,gas%20emitted%20through%20human%20activities.&text=Larger%20image%20to%20save%20or%20printThe%20main%20human%20activity,changes%20also%20emit%20CO2.) Published September 8, 2020. Accessed April 6, 2021.
- [2] Abo BO, Odey EA, Bakayoko M, Kalakodio L. Microalgae to biofuels production: A review on Cultivation, application and renewable energy. <https://doi.org/10.1515/reveh-2018-0052>. Published March 1, 2019. Accessed April 6, 2021.
- [3] “CHBE 464 Lab J Microalgal Cell Culture Problem Statement.” Canvas, canvas.ubc.ca/courses/56631/files/8857714?module_item_id=2026340.
- [4] Sasso S, Stibor H, Mittag M, Grossman AR. The Natural History of Model Organisms: From molecular manipulation of domesticated *Chlamydomonas reinhardtii* to survival in nature. *eLife*. [https://elifesciences.org/articles/39233#:~:text=Chlamydomonas%20reinhardtii%20is%20a%20single,1992%3B%20Rochaix%2C%201995\).](https://elifesciences.org/articles/39233#:~:text=Chlamydomonas%20reinhardtii%20is%20a%20single,1992%3B%20Rochaix%2C%201995).) Published November 1, 2018. Accessed April 8, 2021.
- [5] Almomani FA. Assessment and modeling of microalgae growth considering the effects OF CO₂, nutrients, dissolved organic carbon and solar irradiation. *Journal of Environmental Management*. 2019;247:738-748. doi:10.1016/j.jenvman.2019.06.085
- [6] Khan MI, Shin JH, Kim JD. The promising future of microalgae: current status, challenges, and optimization of a sustainable and renewable industry for biofuels, feed, and other products. *Microbial Cell Factories*. 2018;17(1). doi:10.1186/s12934-018-0879-x
- [7] AL-Mashhadani MKH, Wilkinson SJ, Zimmerman WB. Airlift bioreactor for biological applications with microbubble mediated transport processes. *Chemical Engineering Science*. 2015;137:243-253. doi:10.1016/j.ces.2015.06.032
- [8] de Vree JH, Bosma R, Janssen M, Barbosa MJ, Wijffels RH. Comparison of four outdoor pilot-scale photobioreactors. *Biotechnology for Biofuels*. 2015;8(1). doi:10.1186/s13068-015-0400-2
- [9] Richmond, A., Boussiba, S., Vonshak, A. et al. A new tubular reactor for mass production of microalgae outdoors. *J Appl Phycol* 5, 327–332 (1993). <https://doi-org.ezproxy.library.ubc.ca/10.1007/BF02186235>
- [10] Xu L, Weathers PJ, Xiong X-R, Liu C-Z. Microalgal bioreactors: Challenges and opportunities. *Engineering in Life Sciences*. 2009;9(3):178-189. doi:10.1002/elsc.200800111
- [11] Luna-Brito, Manuel & Sacramento-Rivero, Julio & Baz-Rodríguez, Sergio. (2018). Effects of Medium Composition and Gas Superficial Velocity on Mass Transfer during Microalgae Culturing in a Bubble Column Photobioreactor. *Industrial & Engineering Chemistry Research*. 57. 10.1021/acs.iecr.8b03940.

- [12] Powell, Erin & Mapiour, Majak & Evitts, Richard & Hill, Gordon. (2009). Growth Kinetics of *Chlorella vulgaris* and Its Use as a Cathodic Half Cell. *Bioresource Technology*. 100. 269-274. 10.1016/j.biortech.2008.05.032.
- [13] Yuvraj, Padmanabhan P. Technical insight on the requirements for CO₂-saturated growth of microalgae in photobioreactors. *3 Biotech*. 2017;7(2):119. doi:10.1007/s13205-017-0778-6
- [14] Janssen, M., de Bresser, L., Baijens, T. et al. Scale-up aspects of photobioreactors: effects of mixing-induced light/dark cycles. *Journal of Applied Phycology* 12, 225–237 (2000). <https://doi.org/10.1023/A:1008151526680>
- [15] Boyle, N.R., Morgan, J.A. Flux balance analysis of primary metabolism in *Chlamydomonas reinhardtii*. *BMC Syst Biol* 3, 4 (2009). <https://doi.org/10.1186/1752-0509-3-4>
- [16] Takache, Hosni & Pruvost, Jérémy & Cornet, Jean-François. (2012). Kinetic modeling of the photosynthetic growth of *Chlamydomonas reinhardtii* in a photobioreactor. *Biotechnology progress*. 28. 681-92. 10.1002/btpr.1545.
- [17] Vitova, Milada & Bisova, Katerina & Hlavova, Monika & Kawano, Shigeyuki & Zachleder, Vilem & Čížková, Mária. (2011). *Chlamydomonas reinhardtii*: duration of its cell cycle and phases at growth rates affected by temperature. *Planta*. 234. 599-608. 10.1007/s00425-011-1427-7.
- [18] Yuvraj, Padmanabhan P. Technical insight on the requirements for CO₂-saturated growth of microalgae in photobioreactors. *3 Biotech*. 2017;7(2):119. doi:10.1007/s13205-017-0778-6
- [19] Nonparametric Tests. (n.d.). Retrieved from https://sphweb.bumc.bu.edu/otlt/mph-modules/bs/bs704_nonparametric/BS704_Nonparametric4.html#:~:text=The Mann Whitney U test, sometimes called the Mann Whitney
- [20] Zhan, Jiao & Rong, Junfeng & Wang, Qiang. (2016). Mixotrophic Cultivation, a Preferable Microalgae Cultivation Mode for Biomass/bioenergy Production, and Bioremediation, Advances and Prospect. *International Journal of Hydrogen Energy*. 42. 10.1016/j.ijhydene.2016.12.021.
- [21] Lee, CG. Calculation of light penetration depth in photobioreactors. *Biotechnol. Bioprocess Eng*. 4, 78–81 (1999). <https://doi.org/10.1007/BF02931920>
- [22] Béchet, Quentin & Shilton, Andy & Guieysse, Benoit. (2013). Modeling the effects of light and temperature on algae growth: State of the art and critical assessment for productivity prediction during outdoor cultivation. *Biotechnology advances*. 31. 10.1016/j.biotechadv.2013.08.014.
- [23] Mayerhöfer, Thomas & Popp, Jürgen. (2019). Beer's law derived from electromagnetic theory. *Spectrochimica Acta Part A: Molecular and Biomolecular Spectroscopy*. 215. 10.1016/j.saa.2019.02.103.
- [24] Burgess, Greg & Fernández-Velasco, J & Lovegrove, Keith. (2006). Materials, geometry, and net energy ratio of tubular photobioreactors for microalgal hydrogen production. 16th World Hydrogen Energy Conference 2006, WHEC 2006. 1.

- [25] Huang, Qingshan & Jiang, Fuhua & Wang, Lianzhou & Yang, Chao. (2017). Design of Photobioreactors for Mass Cultivation of Photosynthetic Organisms. *Engineering*. 3. 318-329. 10.1016/J.ENG.2017.03.020.
- [26] Sarker NK, Salam PA. Indoor and outdoor cultivation of *Chlorella vulgaris* and its application in wastewater treatment in a tropical city—Bangkok, Thailand. *SN Applied Sciences*. 2019;1(12). doi:10.1007/s42452-019-1704-9
- [27] Richardson, James & Johnson, Myriah & Joe, Lanter. (2012). Economic comparison of open pond raceways to photo bio-reactors for profitable production of algae for transportation fuels in the Southwest. *Algal Research*. 1. 93–100. 10.1016/j.algal.2012.04.001. *Plants (Basel, Switzerland)*, 9(1), 31. <https://doi.org/10.3390/plants9010031>
- [28] Bošnjaković, Mladen & Sinaga, Nazaruddin. (2020). The Perspective of Large-Scale Production of Algae Biodiesel. *Applied Sciences*. 10. 8181. 10.3390/app10228181.
- [29] Richardson, James & Johnson, Myriah & Zhang, Xuezhi & Zemke, Peter & Chen, Wei & Hu, Qiang. (2014). A financial assessment of two alternative cultivation systems and their contributions to algae biofuel economic viability. *Algal Research*. 4. 10.1016/j.algal.2013.12.003.
- [30] Best Electricity Rates in Canada. Immigroup. <https://www.immigroup.com/news/best-electricity-rates-canada#:~:text=The%20average%20residential%20price%20of,very%20affordable%20by%20global%20standards>. Accessed April 5, 2021.
- [31] Contamination Management in Low-Cost Open Algae Ponds for Biofuels Production Robert C. McBride, Salvador Lopez, Chris Meenach, Mike Burnett, Philip A. Lee, Fiona Nohilly, and Craig Behnke. *Industrial Biotechnology* 2014 10:3, 221-227
- [32] Fernando J. Net Present Value (NPV). Investopedia. <https://www.investopedia.com/terms/n/npv.asp>. Published April 2, 2021. Accessed April 6, 2021.
- [33] W. Sawaengsak, T. Silalertruksa, A. Bangviwat, and S. H. Gheewala, “Life cycle cost of biodiesel production from microalgae in Thailand,” *Energy for Sustainable Development*, vol. 18, pp. 67–74, 2014.
- [34] Y. Zhu, S. B. Jones, and D. B. Anderson, “Algae Farm Cost Model: Considerations for Photobioreactors,” 2018.
- [35] Dębowski, Marcin & Zieliński, Marcin & Kazimierowicz, Joanna & Kujawska, Natalia & Talbierz, Szymon. (2020). Microalgae Cultivation Technologies as an Opportunity for Bioenergetic System Development—Advantages and Limitations. *Sustainability*. 12. 9980. 10.3390/su12239980.
- [36] T. Sarat Chandra, M. Maneesh Kumar, S. Mukherji, V. S. Chauhan, R. Sarada, and S. N. Mudliar, “Comparative life cycle assessment of microalgae-mediated CO₂ capture in open raceway pond and airlift photobioreactor system,” *Clean Technologies and Environmental Policy*, vol. 20, no. 10, pp. 2357–2364, 2018.

- [37] CHBE 488: Carbon Capture, Conversion and Sequestration Technologies. “Carbon Equivalents,” 2021. https://canvas.ubc.ca/courses/26855/pages/week-4-life-cycle-analysis?module_item_id=1902998
- [38] Marsullo, Matteo & Mian, Alberto & Ensinas, Adriano & Manente, Giovanni & Lazzaretto, Andrea & Maréchal, François. (2015). Dynamic Modeling of the Microalgae Cultivation Phase for Energy Production in Open Raceway Ponds and Flat Panel Photobioreactors. *Frontiers in Energy Research*. 3. 10.3389/fenrg.2015.00041.
- [39] de Vree, J.H., Bosma, R., Janssen, M. et al. Comparison of four outdoor pilot-scale photobioreactors. *Biotechnol Biofuels* 8, 215 (2015). <https://doi.org/10.1186/s13068-015-0400-24>
- [40] Marsullo, Matteo & Mian, Alberto & Ensinas, Adriano & Manente, Giovanni & Lazzaretto, Andrea & Maréchal, François. (2015). Dynamic Modeling of the Microalgae Cultivation Phase for Energy Production in Open Raceway Ponds and Flat Panel Photobioreactors. *Frontiers in Energy Research*. 3. 10.3389/fenrg.2015.00041.
- [40] Umen JG, Goodenough UW. Control of cell division by a retinoblastoma protein homolog in *Chlamydomonas*. *Genes Dev*. 2001;15(13):1652-1661. doi:10.1101/gad.892101
- [41] Hosseinizand, Hasti & Sokhansanj, Shahab & Lim, Jim. (2017). Studying the drying mechanism of microalgae *Chlorella vulgaris* and the optimum drying temperature to preserve quality characteristics. *Drying Technology*. 36. 10.1080/07373937.2017.1369986.
- [42] He, Lian & Subramanian, Venkat & Tang, Yinjie. (2012). Experimental analysis and model-based optimization of microalgae growth in photo-bioreactors using flue gas. *Biomass and Bioenergy*. 41. 131–138. 10.1016/j.biombioe.2012.02.025.

Appendix A: Raw Data and Calculated Data

Table A 1: Gas flow rates for each experiment

		Air (L/min)	CO ₂ (L/min)	Total (L/min)
Day 1	High	0.76	0.04	0.8
	Low	0.57	0.03	0.6
	Total (x6)	3.99	0.21	4.2
Day 2	High	0.855	0.045	0.9
	Low	0.665	0.035	0.7
	Total (x6)	4.56	0.24	4.8
Day 3	High	0.57	0.03	0.6
	Low	0.38	0.02	0.4
	Total (x6)	2.85	0.15	3

Table A 2: pH and lighting conditions on first and last day of experiment 1

	First Day			Last Day		
Flask Location	Light Intensity (lux) - 1	Light Intensity (lux) - 2	pH - 1	Light Intensity (lux) - 1	Light Intensity (lux) - 2	pH - 1
A1	7880	7890	6.99	6240	6260	7.1
A2	5780	5780	7.01	5110	5130	7.39
A3	7210	7230	6.96	6680	6680	7.11
B1	7110	7100	7.03	6610	6630	7.25
B2	5750	5750	6.99	4730	4710	7.31
B3	7660	7640	6.95	5330	5330	7.48

Table A 3: pH and lighting conditions on first and last day of experiment 2

	First Day			Last Day		
Flask Location	Light Intensity (lux) - 1	Light Intensity (lux) - 2	pH - 1	Light Intensity (lux) - 1	Light Intensity (lux) - 2	pH - 1
A1	6850	6850	7.05	7580	7550	7.23
A2	5220	5250	6.99	5260	5280	7.31
A3	6730	6720	7.04	6810	6820	7.18
B1	6790	6800	6.95	6470	6500	7.25
B2	5070	5090	7.02	4850	4870	7.27
B3	7720	7720	7.02	7020	7000	7.35

Table A 4: pH and lighting conditions on first and last day of experiment 3

Flask Location	First Day			Last Day		
	Light Intensity (lux) - 1	Light Intensity (lux) - 2	pH - 1	Light Intensity (lux) - 1	Light Intensity (lux) - 2	pH - 1
A1	3860	3860	6.96	3770	3770	7.24
A2	3370	3390	6.94	3050	3070	7.19
A3	5220	5210	6.93	5420	5420	7.25
B1	5260	5260	6.95	5300	5300	7.21
B2	3580	3560	7.01	3280	3280	7.35
B3	4180	4180	7	4240	4240	7.32

Table A 5: Calibration Curve Data

Standard #	V inoculum	V PBS			Average	
	(mL)	(mL)	OD750 #1	OD 750 #2	OD	DCW
1	4	0	0.758	0.764	0.761	0.665
2	3	1	0.588	0.591	0.5895	0.49875
3	2	2	0.403	0.403	0.403	0.3325
4	1.5	2.5	0.353	0.357	0.355	0.24938
5	1	3	0.209	0.213	0.211	0.16625
6	0.8	3.2	0.174	0.174	0.174	0.133
7	0.6	3.4	0.125	0.127	0.126	0.09975
8	0.4	3.6	0.082	0.083	0.0825	0.0665
9	0.2	3.8	0.043	0.044	0.0435	0.03325
10	0	4	0	0	0	0

Figure A 1: Plotted Calibration Curve

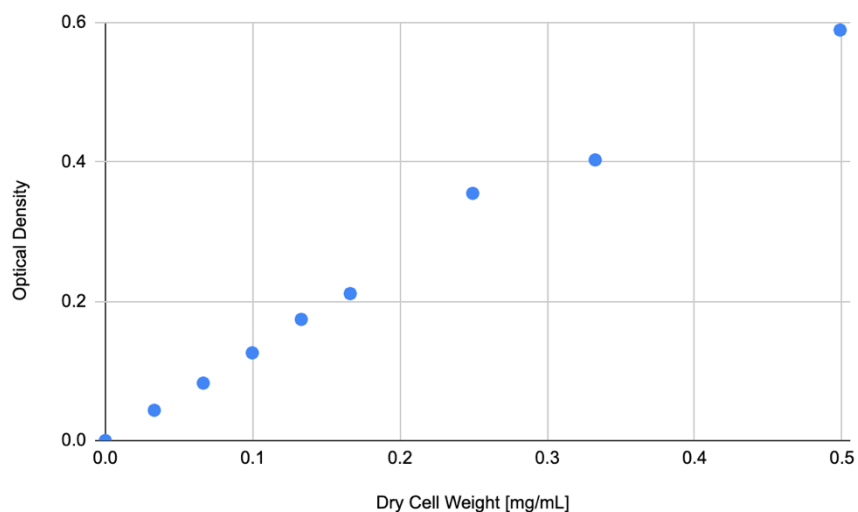


Table A 6: Raw Sampling Data Experiment 1, calculated dry cell weight and uncertainty

	Flask Location	Sample 1	Sample 2	Sample 3	Dilution	Dilution Error	Stdev	Average OD750	DCW	DCW Error
		OD750 Reading 1	OD750 Reading 1	OD750 Reading 1						
Sample 1: 2/4/21	A1	0.007	0.007	0.007	1	0	0	0.007	0.006	1E-04
	A2	0.007	0.006	0.007	1	0	6E-04	0.0067	0.006	6E-04
	A3	0.007	0.007	0.007	1	0	0	0.007	0.006	1E-04
	B1	0.008	0.007	0.007	1	0	6E-04	0.0073	0.006	6E-04
	B2	0.007	0.007	0.006	1	0	6E-04	0.0067	0.006	6E-04
	B3	0.007	0.007	0.007	1	0	0	0.007	0.006	1E-04
Sample 2: 2/8/21	A1	0.657	0.655	0.645	0.25	0.001125	0.006	2.6093	2.192	0.24
	A2	0.534	0.541	0.523	0.25	0.001125	0.009	2.1307	1.79	0.209
	A3	0.601	0.596	0.593	0.25	0.001125	0.004	2.3867	2.005	0.213
	B1	0.571	0.568	0.563	0.25	0.001125	0.004	2.2693	1.907	0.203
	B2	0.531	0.533	0.536	0.25	0.001125	0.003	2.1333	1.792	0.187
	B3	0.667	0.665	0.669	0.25	0.001125	0.002	2.668	2.242	0.23
Sample 3: 2/11/21	A1	0.404	0.406	0.416	0.125	0.0006563	0.006	3.2693	2.747	0.606
	A2	0.321	0.318	0.326	0.125	0.0006563	0.004	2.5733	2.162	0.47
	A3	0.341	0.343	0.341	0.125	0.0006563	0.001	2.7333	2.297	0.478
	B1	0.332	0.329	0.33	0.125	0.0006563	0.002	2.6427	2.22	0.465
	B2	0.297	0.301	0.312	0.125	0.0006563	0.008	2.4267	2.039	0.47
	B3	0.4	0.381	0.393	0.125	0.0006563	0.01	3.1307	2.631	0.603
Sample 4: 2/15/21	A1	0.411	0.4	0.403	0.1	0.00054	0.006	4.0467	3.4	0.924
	A2	0.306	0.325	0.311	0.1	0.00054	0.01	3.14	2.638	0.762
	A3	0.299	0.312	0.294	0.1	0.00054	0.009	3.0167	2.535	0.731
	B1	0.311	0.298	0.306	0.1	0.00054	0.007	3.05	2.563	0.715
	B2	0.327	0.323	0.319	0.1	0.00054	0.004	3.23	2.714	0.733
	B3	0.431	0.418	0.423	0.1	0.00054	0.007	4.24	3.563	0.973
Sample 5: 2/18/21	A1	0.469	0.46	0.447	0.1	0.00054	0.011	4.5867	3.854	1.086
	A2	0.38	0.421	0.387	0.1	0.00054	0.022	3.96	3.327	1.041
	A3	0.416	0.449	0.428	0.1	0.00054	0.017	4.31	3.621	1.073
	B1	0.385	0.341	0.376	0.1	0.00054	0.023	3.6733	3.086	0.99
	B2	0.341	0.362	0.358	0.1	0.00054	0.011	3.5367	2.972	0.859
	B3	0.457	0.491	0.464	0.1	0.00054	0.018	4.7067	3.955	1.169
Sample 6: 2/20/21	A1	0.509	0.516	0.515	0.1	0.00054	0.004	5.1333	4.313	1.143
	A2	0.415	0.411	0.432	0.1	0.00054	0.011	4.1933	3.523	1.001
	A3	0.455	0.421	0.446	0.1	0.00054	0.018	4.4067	3.703	1.102
	B1	0.434	0.459	0.448	0.1	0.00054	0.013	4.47	3.756	1.073
	B2	0.39	0.418	0.45	0.1	0.00054	0.03	4.1933	3.523	1.16
	B3	0.51	0.506	0.499	0.1	0.00054	0.006	5.05	4.243	1.14

Table A 7: Raw Sampling Data Experiment 2, calculated dry cell weight and uncertainty

		Sample 1	Sample 2	Sample 3						
	Flask Location	OD750 Reading 1	OD750 Reading 1	OD750 Reading 1	Dilution	Dilution Error	Stdev	Average		DCW Error
								OD750	DCW	
Sample 1: 2/25/21	A1	0.014	0.012	0.013	1	0	0.001	0.013	0.011	0.001
	A2	0.011	0.011	0.011	1	0	0	0.011	0.009	2E-04
	A3	0.009	0.009	0.009	1	0	0	0.009	0.008	2E-04
	B1	0.01	0.011	0.01	1	0	6E-04	0.0103	0.009	7E-04
	B2	0.01	0.009	0.01	1	0	6E-04	0.0097	0.008	7E-04
	B3	0.009	0.009	0.009	1	0	0	0.009	0.008	2E-04
Sample 2: 3/1/21	A1	0.632	0.641	0.651	0.5	0.0015	0.01	1.2827	1.078	0.066
	A2	0.508	0.514	0.515	0.5	0.0015	0.004	1.0247	0.861	0.047
	A3	0.682	0.689	0.692	0.5	0.0015	0.005	1.3753	1.156	0.063
	B1	0.661	0.667	0.669	0.5	0.0015	0.004	1.3313	1.119	0.059
	B2	0.554	0.566	0.567	0.5	0.0015	0.007	1.1247	0.945	0.056
	B3	0.74	0.741	0.743	0.5	0.0015	0.002	1.4827	1.246	0.061
Sample 3: 3/4/21	A1	0.307	0.305	0.307	0.1	0.00054	0.001	3.0633	2.574	0.673
	A2	0.235	0.234	0.234	0.1	0.00054	6E-04	2.3433	1.969	0.512
	A3	0.277	0.276	0.275	0.1	0.00054	0.001	2.76	2.319	0.606
	B1	0.272	0.273	0.274	0.1	0.00054	0.001	2.73	2.294	0.599
	B2	0.251	0.255	0.25	0.1	0.00054	0.003	2.52	2.117	0.568
	B3	0.306	0.305	0.305	0.1	0.00054	6E-04	3.0533	2.566	0.666
Sample 4: 3/8/21	A1	0.375	0.375	0.373	0.1	0.00054	0.001	3.7433	3.145	0.82
	A2	0.267	0.265	0.265	0.1	0.00054	0.001	2.6567	2.232	0.585
	A3	0.328	0.326	0.323	0.1	0.00054	0.003	3.2567	2.736	0.726
	B1	0.337	0.333	0.335	0.1	0.00054	0.002	3.35	2.815	0.742
	B2	0.297	0.295	0.293	0.1	0.00054	0.002	2.95	2.479	0.655
	B3	0.375	0.375	0.371	0.1	0.00054	0.002	3.7367	3.14	0.828
Sample 5: 3/11/21	A1	0.436	0.436	0.437	0.1	0.00054	6E-04	4.3633	3.666	0.949
	A2	0.32	0.318	0.322	0.1	0.00054	0.002	3.2	2.689	0.709
	A3	0.38	0.382	0.381	0.1	0.00054	0.001	3.81	3.201	0.833
	B1	0.398	0.393	0.397	0.1	0.00054	0.003	3.96	3.327	0.879
	B2	0.349	0.345	0.345	0.1	0.00054	0.002	3.4633	2.91	0.769
	B3	0.425	0.423	0.421	0.1	0.00054	0.002	4.23	3.554	0.932

Table A 8: Raw Sampling Data Experiment 3, calculated dry cell weight and uncertainty

	Flask Location	Sample 1	Sample 2	Sample 3	Dilution	Dilution Error	Stdev	Average OD750	DCW	DCW Error
		OD750 Reading 1	OD750 Reading 1	OD750 Reading 1						
Sample 1: 3/11/21	A1	0.006	0.006	0.006	1	0	0	0.006	0.005	0
	A2	0.006	0.008	0.006	1	0	0.001	0.0067	0.006	0.001
	A3	0.007	0.008	0.007	1	0	6E-04	0.0073	0.006	5E-04
	B1	0.006	0.006	0.006	1	0	0	0.006	0.005	0
	B2	0.006	0.007	0.006	1	0	6E-04	0.0063	0.005	5E-04
	B3	0.006	0.006	0.006	1	0	0	0.006	0.005	0
Sample 2: 3/15/21	A1	0.588	0.586	0.588	1	0	0.001	0.5873	0.494	0.001
	A2	0.432	0.429	0.435	1	0	0.003	0.432	0.363	0.003
	A3	0.656	0.654	0.656	1	0	0.001	0.6553	0.551	0.001
	B1	0.654	0.654	0.655	1	0	6E-04	0.6543	0.55	5E-04
	B2	0.473	0.468	0.471	1	0	0.003	0.4707	0.396	0.002
	B3	0.541	0.542	0.544	1	0	0.002	0.5423	0.456	0.001
Sample 3: 3/18/21	A1	0.598	0.598	0.599	0.5	0.0015	6E-04	1.1967	1.006	0.007
	A2	0.589	0.593	0.591	0.5	0.0015	0.002	1.182	0.993	0.009
	A3	0.682	0.688	0.689	0.5	0.0015	0.004	1.3727	1.153	0.013
	B1	0.722	0.722	0.729	0.5	0.0015	0.004	1.4487	1.217	0.014
	B2	0.609	0.612	0.609	0.5	0.0015	0.002	1.22	1.025	0.009
	B3	0.643	0.639	0.64	0.5	0.0015	0.002	1.2813	1.077	0.01
Sample 4: 3/22/21	A1	0.337	0.336	0.336	0.2	0.00096	6E-04	1.6817	1.413	0.036
	A2	0.337	0.336	0.336	0.2	0.00096	6E-04	1.6817	1.413	0.036
	A3	0.412	0.411	0.413	0.2	0.00096	0.001	2.06	1.731	0.046
	B1	0.43	0.427	0.422	0.2	0.00096	0.004	2.1317	1.791	0.06
	B2	0.355	0.36	0.352	0.2	0.00096	0.004	1.7783	1.494	0.053
	B3	0.372	0.367	0.369	0.2	0.00096	0.003	1.8467	1.552	0.048
Sample 4: 3/26/21	A1	0.321	0.326	0.326	0.2	0.00096	0.003	1.6217	1.363	0.045
	A2	0.316	0.319	0.317	0.2	0.00096	0.002	1.5867	1.333	0.038
	A3	0.441	0.439	0.438	0.2	0.00096	0.002	2.1967	1.846	0.051
	B1	0.462	0.459	0.457	0.2	0.00096	0.003	2.2967	1.93	0.057
	B2	0.365	0.365	0.363	0.2	0.00096	0.001	1.8217	1.531	0.042
	B3	0.38	0.38	0.389	0.2	0.00096	0.005	1.915	1.609	0.06

Table A 9: Calibration Curve Specifications

Slope	y-intercept	R ²
1.190	0	0.996

Figure A 2: Average Cell Growth Curve

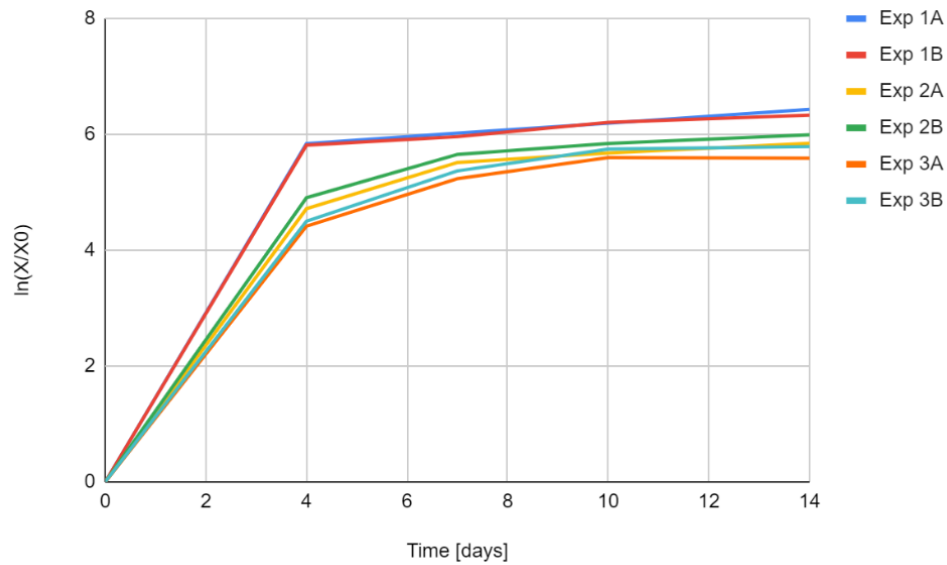


Table A 10: Data for Cell Growth Curve

	Day	A1	A2	A3	Average	B1	B2	B3	Average
Experiment 1	0	0	0	0	0	0	0	0	0
	4	5.92094	5.76707	5.831743	5.839918	5.734811	5.768321	5.943174	5.815435
	7	6.146431	5.955837	5.967367	6.023212	5.887114	5.897154	6.103091	5.962453
	10	6.359739	6.154858	6.065998	6.193531	6.030467	6.183117	6.406408	6.206664
	14	6.484999	6.386879	6.422783	6.431554	6.216425	6.27382	6.510825	6.33369
Experiment 2	0	0	0	0	0	0	0	0	0
	4	4.591747	4.534227	5.029227	4.7184	4.858561	4.756558	5.104373	4.906498
	7	5.46231	5.361434	5.725761	5.516502	5.576682	5.563331	5.826765	5.655592
	10	5.662782	5.486932	5.891235	5.680316	5.781341	5.720877	6.028725	5.843647
	14	5.816042	5.673011	6.04816	5.845738	5.948624	5.881303	6.152733	5.99422
Experiment 3	0	0	0	0	0	0	0	0	0
	4	4.583833	4.171306	4.492714	4.415951	4.691857	4.308323	4.504121	4.501434
	7	5.295536	5.177843	5.23208	5.235153	5.486639	5.260779	5.363897	5.370439
	10	5.635781	5.530421	5.638031	5.601411	5.8729	5.637605	5.729378	5.746628
	14	5.59945	5.472271	5.702266	5.591329	5.947455	5.66168	5.765713	5.791616

Figure A 3: Plot of Cell Concentration versus Time

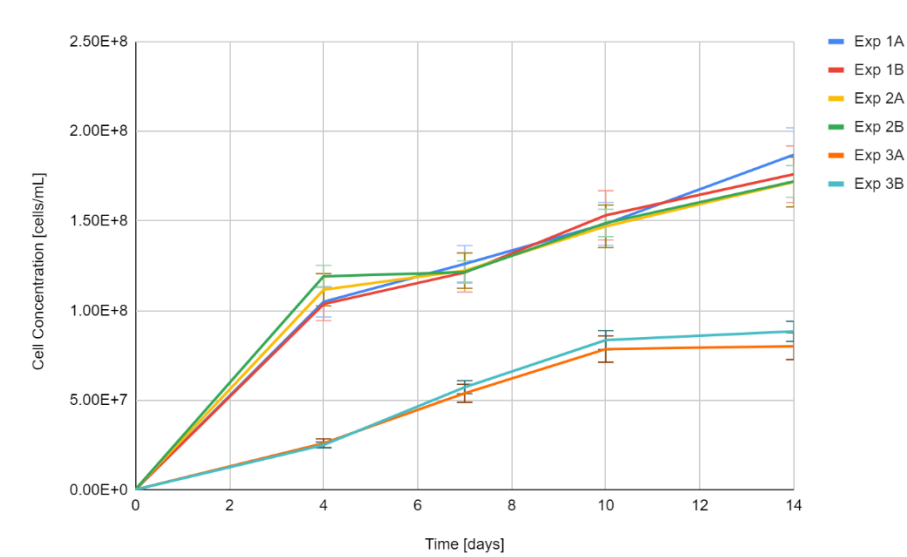


Table A 11: Values of Maximum Biomass Density

	Max Density	Stdev
1A	3.6	0.431736
1B	4	0.344597
2A	3.4	0.328753
2B	3.4	0.160416
3A	1.6	0.341626
3B	1.8	0.226761

Figure A 4: Plot of Penetration Depth versus Cell Concentration

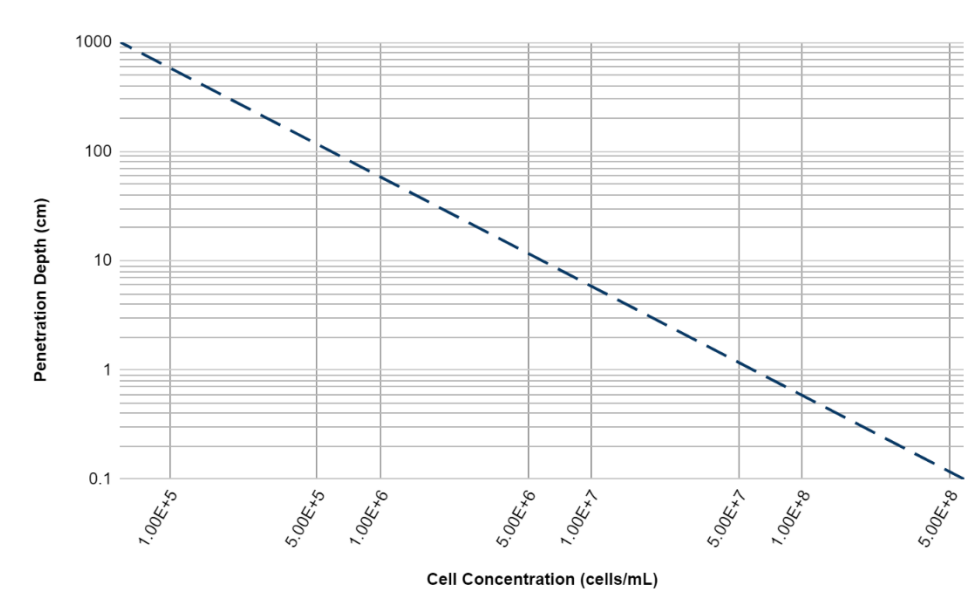


Table A 12: Data used for plot of penetration depth versus cell concentration

Cell Concentration	Penetration Depth
584295144.3	0.1
58429514.43	1
5842951.443	10
584295.1443	100
58429.51443	1000

Figure A 5: Plot of percent saturation of carbon dioxide versus k_La

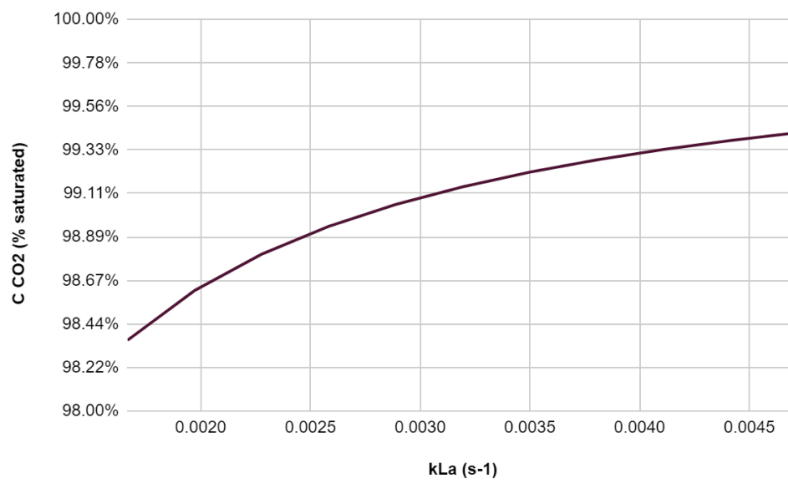


Table A 13: Data used in Figure A5

Max Gas Flow	
k_La	C CO2 (% saturated)
0.00167	98.36
0.00197	98.61
0.00228	98.80
0.00258	98.94
0.00289	99.05
0.00319	99.14
0.0035	99.22
0.00381	99.28
0.00411	99.34
0.00442	99.38
0.00472	99.42

Table A 14: Equipment Costs

Equipment	Cost per unit
Air pump	\$ 8.53
Lamps	\$ 9.30
Bulb	\$ 2.74
Air conditioner	\$ 463.27

Table A 15: Other data used in cost calculations

1 USD =	32.81	THB
Electricity Price	0.00012	\$/Wh
Price of microalgal biomass	0.0003	\$/g
Density of CO ₂	1.8	kg/m ³

Table A 16: Capital Costs Calculated

	Indoor Airlift Reactor	Outdoor Tubular Reactor	Outdoor Raceway Pond
Air pump	\$8.53	\$8.53	\$ -
Lamps	\$171.81	\$ -	\$ -
Bulb	\$50.70	\$ -	\$ -
Air conditioner	\$463.27	\$ -	\$ -
Capital cost (\$)	\$694.31	\$8.53	\$ -

Table A 17: Operating Costs Calculated

	Indoor Airlift Reactor	Outdoor Tubular Reactor	Outdoor Raceway Pond
Air pump energy consumption (Wh/day)	0.549	0.549	0
Air pump energy cost (\$/yr)	\$0.02	\$0.02	\$ -
Light energy consumption (Wh/day)	3006	0	0
Lighting costs (\$/yr)	\$120.94	\$ -	\$ -
Temperature control energy consumption (Wh/day)	106.6	0	0
Temperature control costs (\$/yr)	\$4.29	\$ -	\$ -
Total energy consumption (Wh/day)	3113.2	0.6	0
Total energy cost (\$/day)	\$0.38	\$0.00	\$ -
Operating cost (\$/yr)	\$125.25	\$0.02	\$ -

Table A 18: Revenues Calculated

	Indoor Airlift Reactor	Outdoor Tubular Reactor	Outdoor Raceway Pond
Operating days	14	14	14
Biomass produced from all 6 flasks (g)	112.08	94.03	46.71
Price biomass (\$/g)	\$0.00	\$0.00	\$0.00
Revenues (\$/batch)	\$0.00	\$0.00	\$0.00

Table A 19: NPW Calculation

	Indoor Airlift Reactor	Outdoor Tubular Reactor	Outdoor Raceway Pond
Capital costs	\$694.31	\$8.53	\$0.00
Operating costs (\$/year)	\$125.25	\$0.02	\$0.00
Revenue (\$/year)	\$0.06	\$0.05	\$0.02
Lifetime (years)	\$15.00	\$15.00	\$15.00
i	10.00%	10.00%	10.00%
NPW	-\$519.29	-\$8.14	\$0.18

Table A 20: Carbon Pricing Calculations

	Indoor Airlift Reactor	Outdoor Tubular Reactor	Outdoor Raceway Pond
Total energy consumption (Wh/day)	3113.18	0.55	0
CO ₂ emissions rate from energy consumption (kg CO ₂ /kWh)	0.41	0.41	0.41
CO ₂ emissions (kg CO ₂ /year)	421.21	0.07	0
Carbon tax (\$/tonne CO ₂)	30	30	30
Carbon tax (\$/year)	12.64	0	0
Total CO ₂ consumed (kg/year)	179.63	205.29	128.3
Net CO ₂ emissions	241.59	-205.21	-128.3

Appendix D: Daily Work Plans

Day 1 Work Plan

The first experimental day is dedicated to the indoor airlift bioreactor set up.

Media Preparation:

- Prepare 4 L of TAP media.
- Add 800 mL of TAP media to 6x1L flasks.
- Autoclave culture flasks and let cool.

Inoculation and Sampling:

- Take an absorbance reading of the *C. reinhardtii* inoculum, and record the value. This should be the same for all three experimental days to ensure constant initial cell density. Gently mix the sample with the pipette right before the reading to reduce settling.
- Inoculate each flask with 5 mL of parent culture in hood using sterile method once they have cooled to room temperature

Reactor Setup and Sampling After Day 1:

- Connect the 1L flasks to the aeration system according to Figure 4.
- Turn on all 6 lights and measure and record the light intensity within the lightbox at each flask placement.
- Set the temperature to 30°C.
- Set aeration for 1A, 1B, 1C to 1.1 L/min and 2A, 2B, 2C to 1.6 L/min.
- Ensure that the inlet gas reaches each flask by observing bubbles.
- Record any general observations throughout the experimental run.
- Collect samples on Mondays and Thursdays in triplicates for the duration of the trial run. Gently mix the samples in the cuvette with a pipette before taking the absorbance. Run each sample through the spectrophotometer once. If the samples are found to be identical proceed with only one sample drawn.
- Take pictures of the flasks in the lightbox when sampling.
- At the end of the 2 week experiment, check the pH for CO₂ induced acidity using a pH analyzer.
- Analyse samples by comparing to literature calibration curve or to a borrowed calibration curve from another team.
- At the end of the 2 week run, dispose of the sample by either combining with a bleach solution or autoclaving then pouring down the sink.

Day 2 Work Plan

The goal for day 2 is to simulate the conditions found in an outdoor tubular photobioreactor.

Media Preparation:

- Prepare 4 L of TAP media.
- Add 800 mL of TAP media to 6x1L flasks.
- Autoclave culture flasks and let cool.

Inoculation and Sampling:

- Take an absorbance reading of the *C. reinhardtii* inoculum, and record the value. This should be the same for all three experimental days to ensure constant initial cell density. Gently mix the sample with the pipette right before the reading to reduce settling.
 - If needed, dilute the inoculum with fresh media to match the absorbance reading taken at the beginning of the semester.
- Inoculate each flask with 10 mL of parent culture in hood using sterile method once they have cooled to room temperature

Reactor Setup and Sampling After Day 1:

- Connect the 1L flasks to the aeration system according to Figure 4.
- Turn on all 6 lights and measure and record the light intensity within the lightbox at each flask placement. Set the timer such that lights are on for 14 hr/day.
- Ensure the thermostat is switched off for the duration of the experiment.
- Set aeration for 1A, 1B, 1C to 0.7 L/min and 2A, 2B, 2C to 0.9 L/min.
- Ensure that the inlet gas reaches each flask by observing bubbles.
- Record any general observations throughout the experimental run.
- Collect one sample from each flask on Mondays and Thursdays for the duration of the trial run. Gently mix the samples in the cuvette with a pipette before taking the absorbance. Run each sample through the spectrophotometer once.
- Take pictures of the flasks in the lightbox when sampling.
- At the end of the 2 week experiment, check the pH for CO₂ induced acidity using a pH analyzer.
- Analyse samples by comparing to literature calibration curve or to a borrowed calibration curve from another team.
- At the end of the 2 week run, dispose of the sample by either combining with a bleach solution or autoclaving then pouring down the sink.

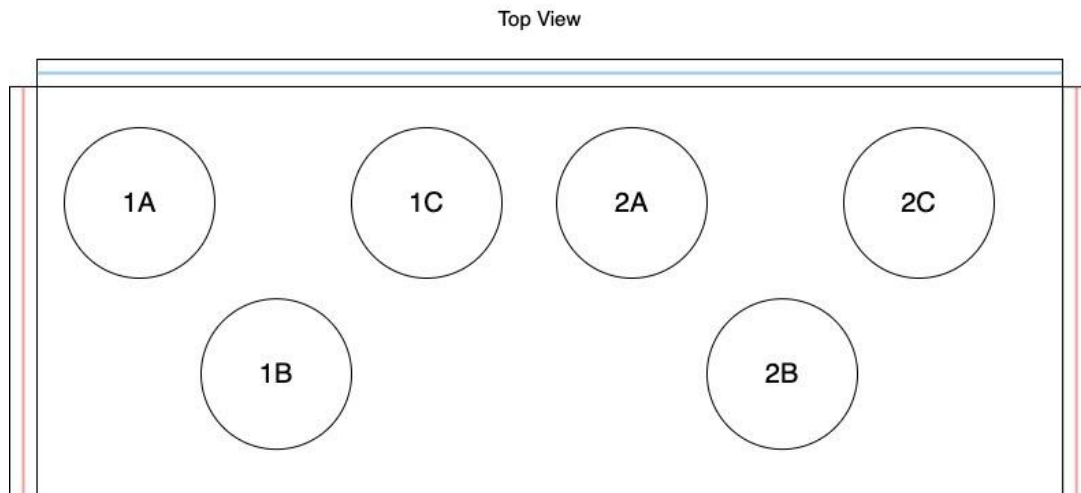


Figure 1: Schematic of experimental apparatus inside the light chamber. Lights shown in red are switched off while lights in blue are switched on

		Air (L/min)	Co2 (L/min)	Total (L/min)
	High	0.855	0.045	0.9
	Low	0.665	0.035	0.7
Day 2	Total (x6)	4.56	0.24	4.8

Figure 2: Air flows for experimental apparatus on day 2

Day 3 Work Plan

The goal for day 3 is to simulate the conditions found in an outdoor raceway pond.

Media Preparation:

- Prepare 4 L of TAP media.
- Add 800 mL of TAP media to 6x1L flasks.
- Autoclave culture flasks and let cool.

Inoculation and Sampling:

- Take an absorbance reading of the *C. reinhardtii* inoculum, and record the value. This should be the same for all three experimental days to ensure constant initial cell density. Gently mix the sample with the pipette right before the reading to reduce settling.
 - If needed, dilute the inoculum with fresh media to match the absorbance reading taken at the beginning of the semester.
- Inoculate each flask with 10 mL of parent culture in hood using sterile method once they have cooled to room temperature

Reactor Setup and Sampling After Day 1:

- Connect the 1L flasks to the aeration system according to Figure 4.
- Turn on 2 lights as shown in Figure 1 and measure and record the light intensity within the lightbox at each flask placement. Set the timer such that lights are on for 14 hr/day.
- Ensure the thermostat is switched off for the duration of the experiment.
- Set aeration for 1A, 1B, 1C to the 'Low' conditions and 2A, 2B, 2C to the 'High' conditions listed in Figure 2 below.
- Ensure that the inlet gas reaches each flask by observing bubbles.
 - If no bubbles are observed, increase gas flow rate (both air and CO₂ to maintain the same CO₂:air ratio) until bubbles are observed. Record new flow rates.
- Record any general observations throughout the experimental run.
- Collect one sample from each flask on Mondays and Thursdays for the duration of the trial run. Gently mix the samples in the cuvette with a pipette before taking the absorbance. Run each sample through the spectrophotometer once.
- Take pictures of the flasks in the lightbox when sampling.
- At the end of the 2 week experiment, check the pH for CO₂ induced acidity using a pH analyzer.
- Analyse samples by comparing to literature calibration curve or to a borrowed calibration curve from another team.
- At the end of the 2 week run, dispose of the sample by either combining with a bleach solution or autoclaving then pouring down the sink.

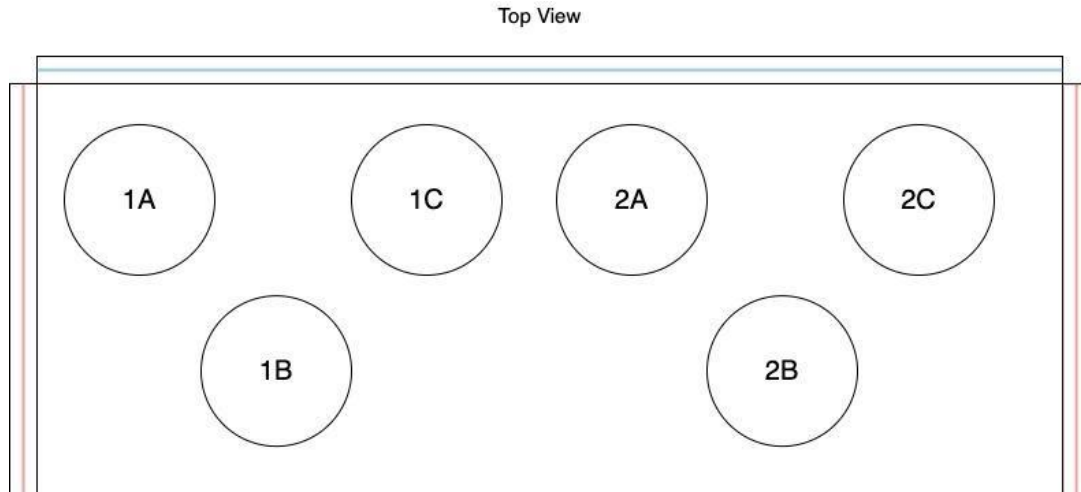


Figure 1: Schematic of experimental apparatus inside the light chamber. Lights shown in red are switched off while lights in blue are switched on

		Air (L/min)	CO ₂ (L/min)	Total (L/min)
	High	0.57	0.03	0.6
	Low	0.38	0.02	0.4
Day 3	Total (x6)	2.85	0.15	3

Figure 2: Air flows for experimental apparatus on day 3